Effects
of magnetic reconnection

Bipolar X-point Reconnection

Bipolar 2D Reconnection (Arcade)

Tripolar X-point Reconnection

Fan Reconnection

Quadrupolar X-point Reconnection

Spine Reconnection

Volume of field-line shrinking (relaxation) after magn. Reconnection defines geometry of acceleration region :

-cusps
-double cusps
-jets
-curved hybperboloids
-spines

Effects of magnetic reconnection

Global topology and connectivity of the field lines change,

Magnetic energy is converted to heat, kinetic energy, and fast particles.

Large currents, electric fields and shock waves are generated which help to accelerate particles.

Most strong particle acceleration occurs during the impulsive phase and it is most obviously characterised by impulsive hard X-rays (HXR) and microwave emission which implies the presence of accelerated electrons.

HXR emission (photon energies > 10 keV) occurs in impulsive bursts, fractions of seconds long. It correlates well with impulsive microwave radio emission in the 3-10 GHz range.

Both HXR and microwaves **show complex fluctuations on short timescales,** implying multiple short acceleration bursts.

Large-scale electric field
in Sweet-Parker current sheet

Small-scale electric fields
in magnetic X and O points
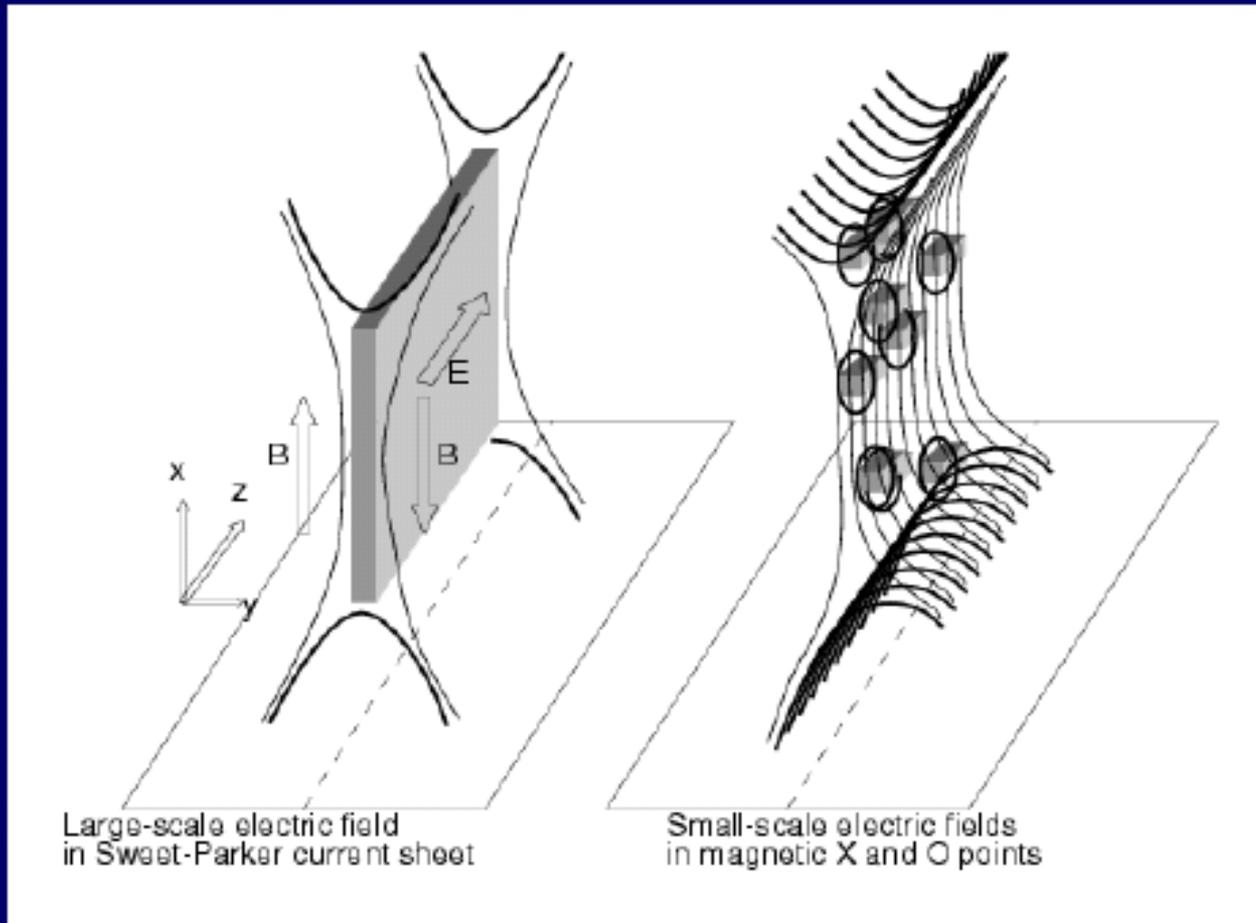
Fast (subsecond) time structures of hard X-ray and radio pulses in solar flares suggest small-scale, fragmented, bursty magnetic reconnection mode.

Magnetic field B ⟵
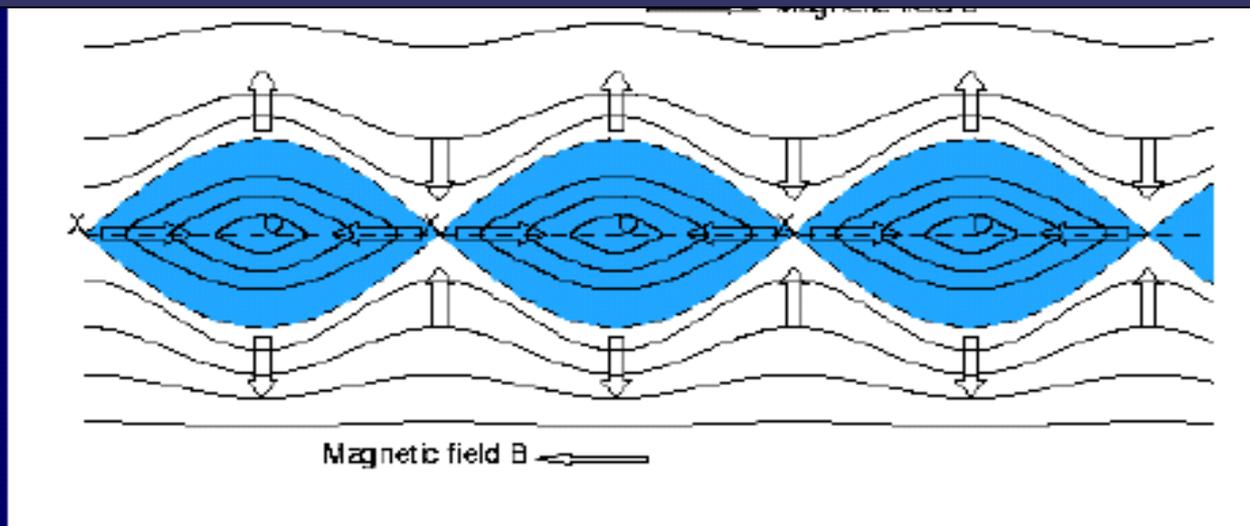
Magnetic island formation by tearing mode instability
(Furth, Killeen, & Rosenbouth et al. 1963)

Magnetic X-point and O-points form →
coalescence instability (Pritchett & Wu 1979)

Magnetic island formation + coalescence instability →
regime of impulsive bursty reconnection
(Leboef et al. 1982; Tajima et al. 1987; Kliem 1998, 1995)

# About energetic particles: electric field acceleration or stochastic acceleration, such as by shocks?
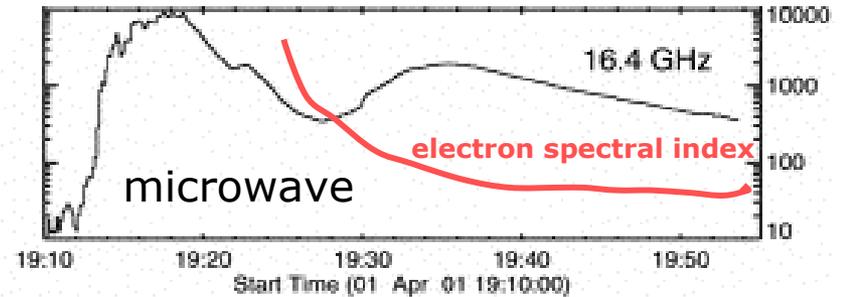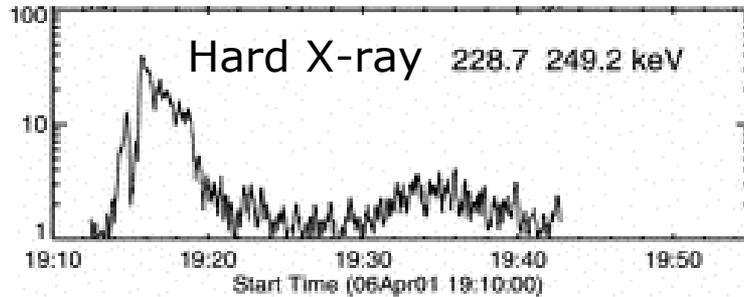
1.
particle acceleration by electric field and then collapsing magnetic traps

(Somov & Kosugi 1997)

Evolving magnetic traps form between shock fronts and closed magnetic loops formed by successive magnetic reconnection.

Pre-accelerated (by electric field) electrons are further accelerated in the traps via a first Fermi mechanism, and then precipitate to emit at foot-points.
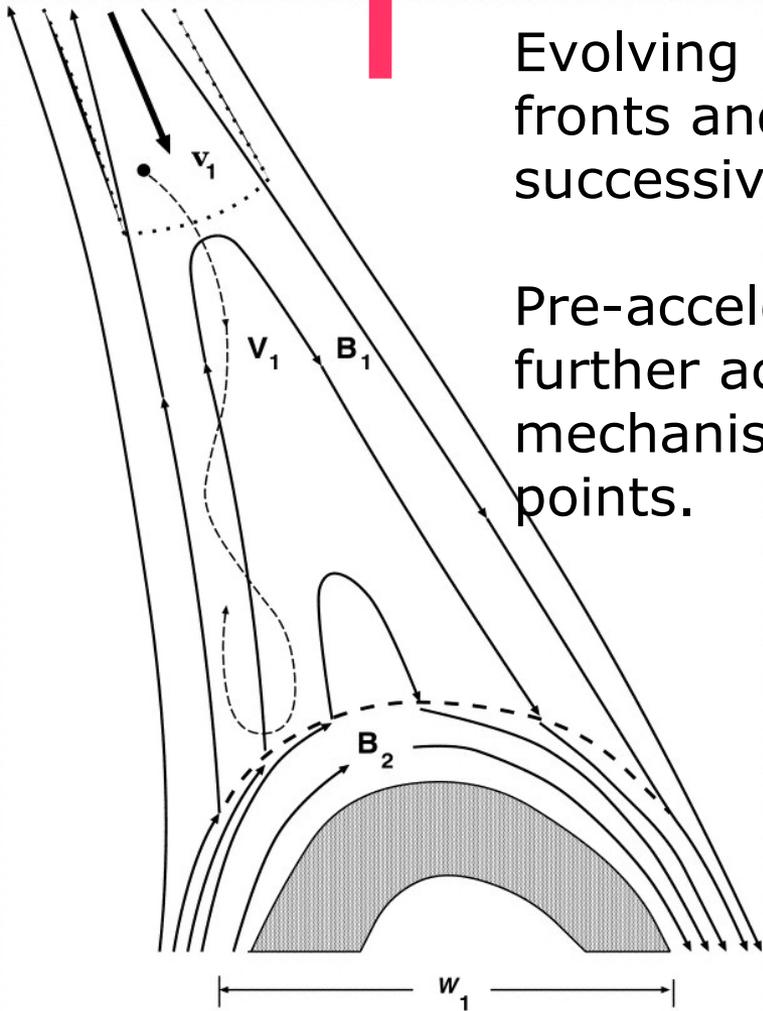
-Diffusive (second-order Fermi) (multiple shock crossings)

2.

SHOCK

e-

e-

upstream   downstream
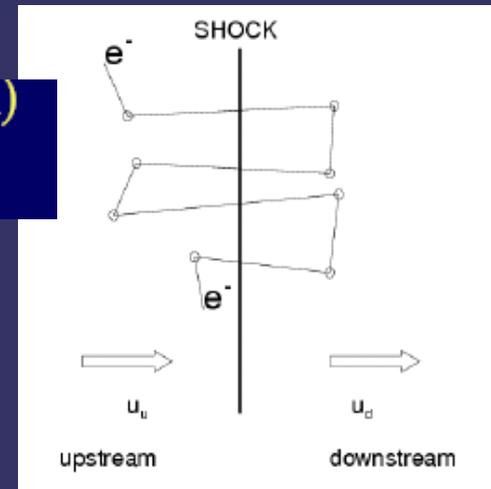
PARTICLE ACCELERATION IN SOLAR FLARES

1) Magnetic topology of acceleration region
2) Geometry of acceleration region
3) Dynamics of acceleration region
4) Accelerating electromagnetic fields
5) Particle kinematics
6) Hard X-ray and radio emission

Refs : a) Aschwanden M.J. 2002, Space Science Reviews, Vol. 101, p.1-227
"Particle Acceleration and Kinematics in Solar Flares"
b) Aschwanden M.J. 2004, PRAXIS Publishing, Chichester, UK
& Springer, Berlin, 850p, (in press)
"Physics of the Solar Corona. An Introduction"

Book online: http://www.lmsal.com/~aschwand/

Flare radiation and emission mechanisms

Radio – microwave to metre wavelengths, produced by **gyrosynchrotron, bremsstrahlung** and collective plasma processes.

Optical emission – lines and continua, Hα line is seen in emission (due to collisional excitation in hot, flare-produced plasma).

White-light continua are probably produced by hydrogen recombination following electron bombardment and H$^-$ emission.

UV lines and continua – excitation by hot flare-produced plasma, with an "impulsive contribution" due to nonthermal electrons.

Flare radiation and emission mechanisms (contd.)

- **EUV line emission**.

- **Soft X-ray – lines and continua** (<u>thermal e^- - p^+ bremsstrahlung</u>, bound-free continuum).

- **Hard X-rays**– <u>non-thermal e^- - p^+ bremsstrahlung</u>.

∀**γ-ray lines and continua**:
  - continuum up to 1 MeV produced by non-relativistic electron bremsstrahlung
  - >10 MeV continuum is due to relativistic electron bremsstrahlung.

# Flare radiation and emission mechanisms (contd.)

γ-ray emission (contd.)

- narrow lines in 4-7 MeV range produced when accelerated p^+ and α particles interact with ambient heavy nuclei.

- **strongest γ-ray line** is the neutron capture line at **2.23 MeV**, with another strong line at **0.511 MeV** due to positron annihilation.

Svestka 1976

TRAJECTORY OF TRAPPED PARTICLE

MIRROR POINT
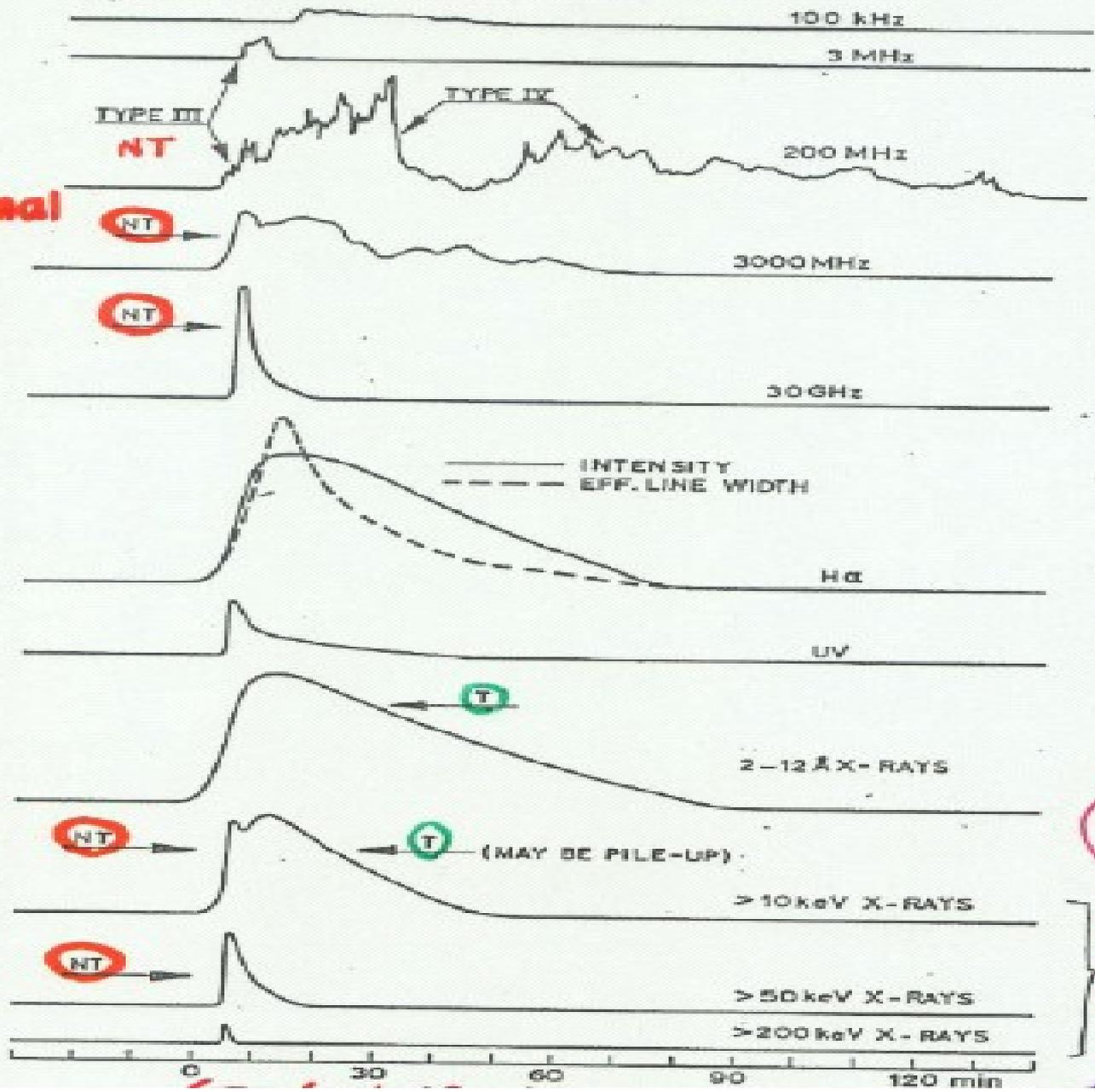
MAGNETIC FIELD LINE
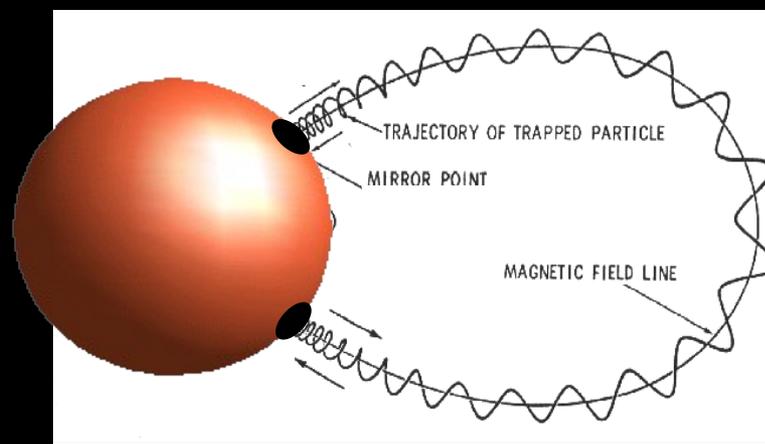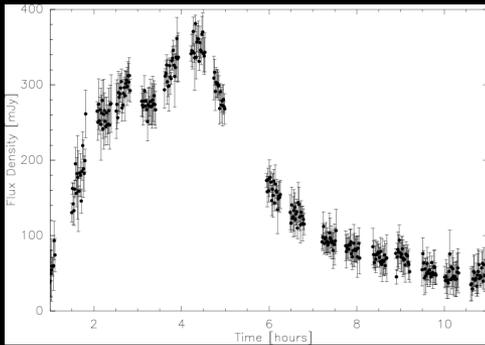
Magnetic field

by synchrotron radiation

Electron

Emitted Photons

Magnetic Field Line
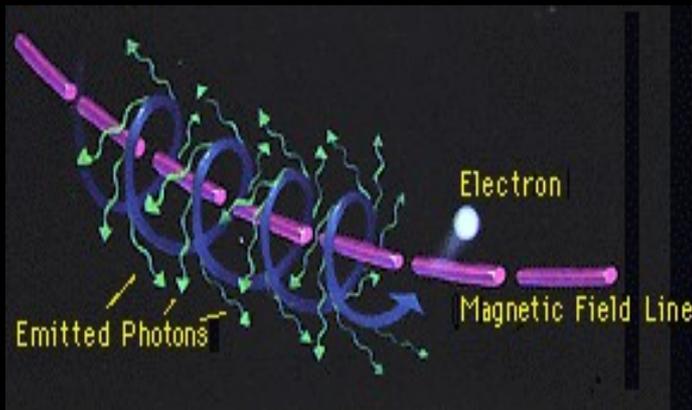
Matter

Bremsstrahlung emission

The Production of X-rays in Solar Flares

Accelerated Electron

Proton

X-ray Photon
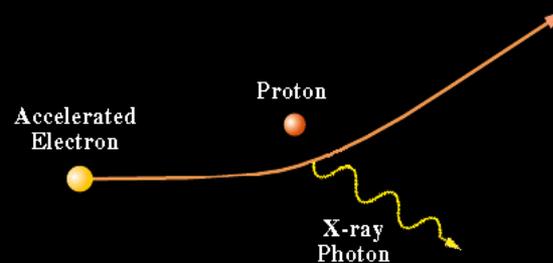
Radiation field

Inverse Compton scattering

$e-$

$e-$

ν'

ν

$\nu' > \nu$
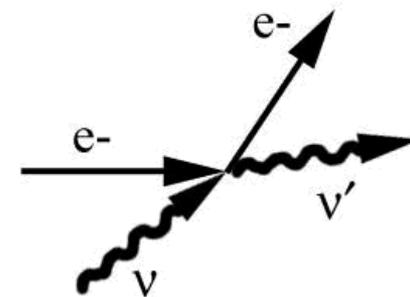
High energy e- initially
e- loses energy

Emission Mechanisms

- Inverse Compton Radiation

- Synchrotron Radiation

- bremsstrahlung

Radiative transfer equation

- transfer equation: emission

I_v ds $I_v + dI_v$

Increment in
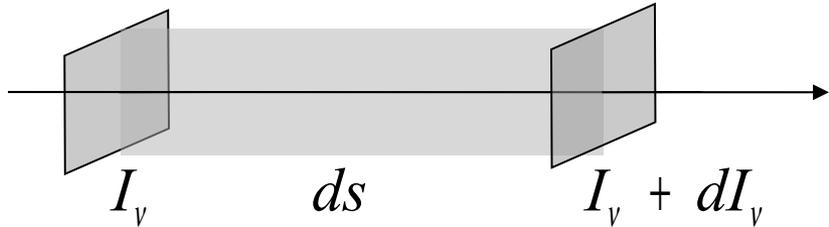
Intensity

Energy added to the ray:

is proportional to path element:

emission coefficient j

$$dE = + dI_v \, dv \, dt \, d\omega \, dA$$

$$ds$$

$$\boxed{dI_v = j \, ds}$$

Radiative Transfer Equation

The specific intensity of radiation is the energy flux per unit time, unit frequency, unit solid angle and unit area normal to the direction of propagation.

The radiative transfer equation states that the specific intensity of radiation I_σ during its propagation in a medium is subject to losses due to extinction and to gains due to emission:

$$\frac{dI_\sigma}{dx} = -\mu_\sigma \cdot I_\sigma + \rho \cdot j_\sigma$$

where x is the co-ordinate along the optical path, μ_σ is the extinction coefficient, ρ is the mass density j_σ is the emission coefficient per unit mass.

Bruno Carli , IFAC

frequency σ

A Simple Case

- no scattering effect,

- local thermodynamic equilibrium,

- homogeneous medium.

Interaction radiation – matter

Energy can be removed from, or delivered to, the radiation field

Classification by physical processes:

True absorption: photon is destroyed, energy is transferred into kinetic energy of gas

True emission: photon is generated, extracts kinetic energy from the gas

Scattering: photon interacts with scatterer
→ direction changed
→ no energy exchange with gas

Extinction

In general, the extinction coefficient μ_σ includes both the absorption coefficient α_σ and the scattering coefficient s_σ,

$$\mu_\sigma = \alpha_\sigma + s_\sigma$$

In the case of a pure gas atmosphere with no-scattering a simple expression is obtained:

$$\mu_\sigma = \alpha_\sigma$$

Emission

In absence of scattering and for local thermodynamic equilibrium (LTE), the source function is equal to :

$$\rho \cdot j_\sigma = \alpha_\sigma B_\sigma (T)$$

where α_σ is the absorption coefficient (equal to the emission coefficient for the Kirchhoff's law) and $B_\sigma(T)$ is the Plank function at frequency σ and temperature T.

$$B_\sigma(T) = \frac{2h\nu\sigma^3}{c^2} \frac{1}{e^{h\nu\sigma/kT} - 1}$$

Radiative Transfer Equation
for LTE and No Scattering

For an atmosphere with no scattering and in LTE the radiative transfer equation is reduced to:

$$\frac{dI_\sigma}{dx} = -\alpha_\sigma \cdot I_\sigma + \alpha_\sigma \cdot B_\sigma(T)$$

Analytical Solution of the Integral
Homogeneous Medium

An analytical integral expression of the differential equation of radiative transfer:

$$\frac{dI_\sigma}{dx} = -\alpha_\sigma \cdot I_\sigma + \alpha_\sigma \cdot B_\sigma(T)$$

can only be obtained for an homogeneous medium.

Analytical Solution of the Integral
Homogeneous Medium

The differential equation is at point x and we want to obtain the integral from x_1 and x_2.
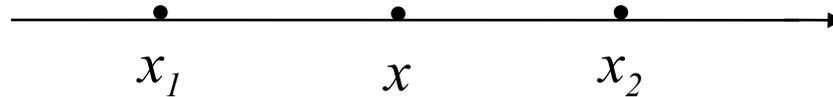
This can be formally obtained multiplying both terms of the differential equation by $exp[\alpha_\sigma(x-x_1)]$ (i.e. the attenuation from x_1 to x).

$$e^{\alpha_\sigma (x-x_1)} \cdot \frac{dI_\sigma}{dx} = \alpha_\sigma \cdot e^{\alpha_\sigma (x-x_1)} \cdot [-I_\sigma + \cdot B_\sigma (T)]$$

$$e^{\alpha_\sigma (x-x_1)} \cdot \frac{dI_\sigma}{dx} + \alpha_\sigma \cdot e^{\alpha_\sigma (x-x_1)} \cdot I_\sigma = \alpha_\sigma \cdot e^{\alpha_\sigma (x-x_1)} \cdot B_\sigma (T)$$

$$\frac{d}{dx}\left[e^{\alpha_\sigma (x-x_1)} \cdot I_\sigma \right] = \alpha_\sigma \cdot e^{\alpha_\sigma (x-x_1)} \cdot B_\sigma (T)$$

An expression is obtained that can be integrated from x_1 to x_2.

$$e^{\alpha_\sigma (x_2-x_1)} \cdot I_\sigma (x_2) - e^{\alpha_\sigma (x_1-x_1)} \cdot I_\sigma (x_1) = \left(e^{\alpha_\sigma (x_2-x_1)} - e^{\alpha_\sigma (x_1-x_1)} \right) \cdot B_\sigma (T)$$

$$e^{\alpha_\sigma (x_2-x_1)} \cdot I_\sigma (x_2) = I_\sigma (x_1) + B_\sigma (T) \cdot \left(e^{\alpha_\sigma (x_2-x_1)} - 1 \right)$$

$$I_\sigma (x_2) = I_\sigma (x_1) \cdot e^{-\alpha_\sigma (x_2-x_1)} + B_\sigma (T) \cdot \left(1 - e^{-\alpha_\sigma (x_2-x_1)} \right)$$

Analytical Solution of the Integral
Homogeneous Medium

In the integral expression of radiative transfer:

$$I_\sigma \left(x_2 \right) = I_\sigma \left(x_1 \right) \cdot e^{-\alpha_\sigma (x_2 - x_1)} + B_\sigma (T) \cdot \left[1 - e^{-\alpha_\sigma (x_2 - x_1)} \right]$$

the first term is the Lambert-Beer law which gives the attenuation of the external source and the second term gives the emission of the local source.

When the optical and physical properties of the medium are not constant along the optical path, the absorption coefficient $\alpha_\sigma(x)$ and the local temperature $T(x)$ depend on the variable of integration x. In general, for an inhomogeneous medium the differential equation cannot be analytically integrated.

Integral equation of Radiative Transfer
variable medium

Intensity of the background source

"Transmittance" between 0 and L

"Transmittance" between l and L

$$I_\sigma(L) = I_\sigma(0) e^{-\tau_\sigma(0,L)} + \int_0^{\tau_\sigma(0,L)} B_\sigma(T(x)) e^{-\tau_\sigma(x,L)} d\tau_\sigma$$

Spectral intensity observed at L

Absorption term

Emission term

"Optical depth" $\longrightarrow$ $\tau_\sigma(x,L) = \int_x^L \alpha_\sigma(x') dx'$

Radio Flares
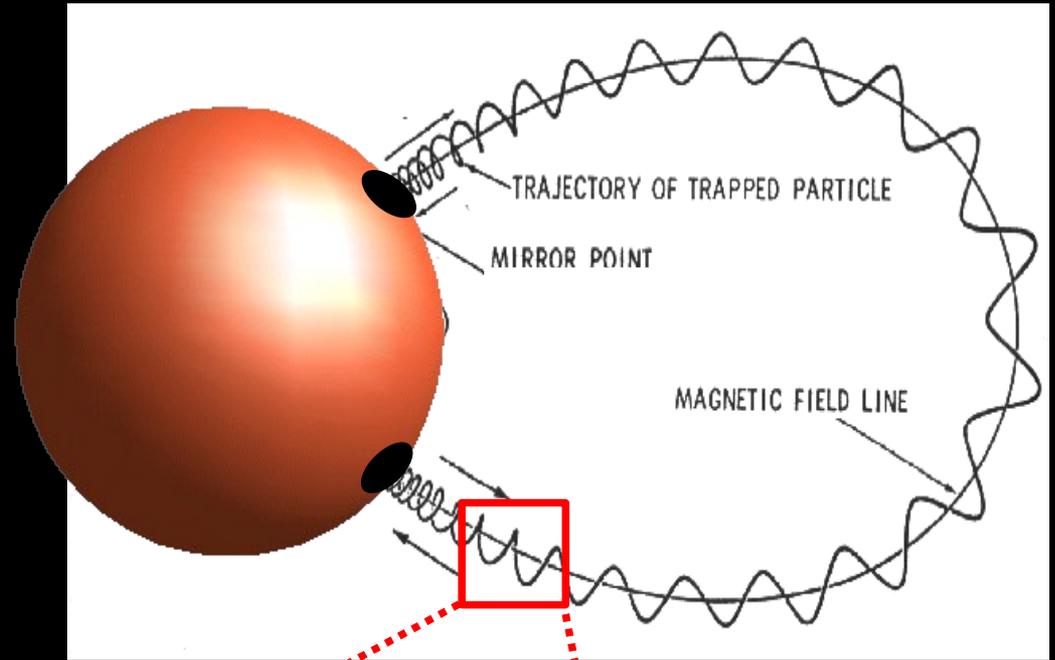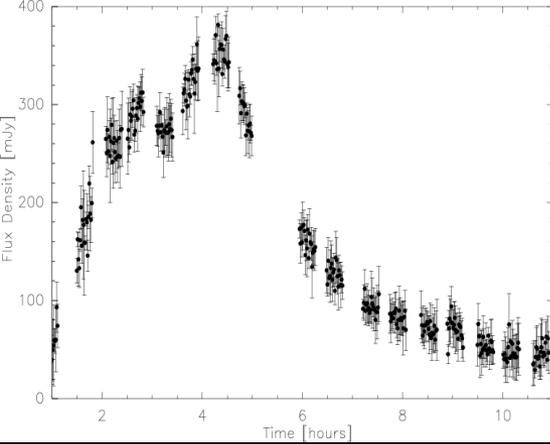
Synchrotron
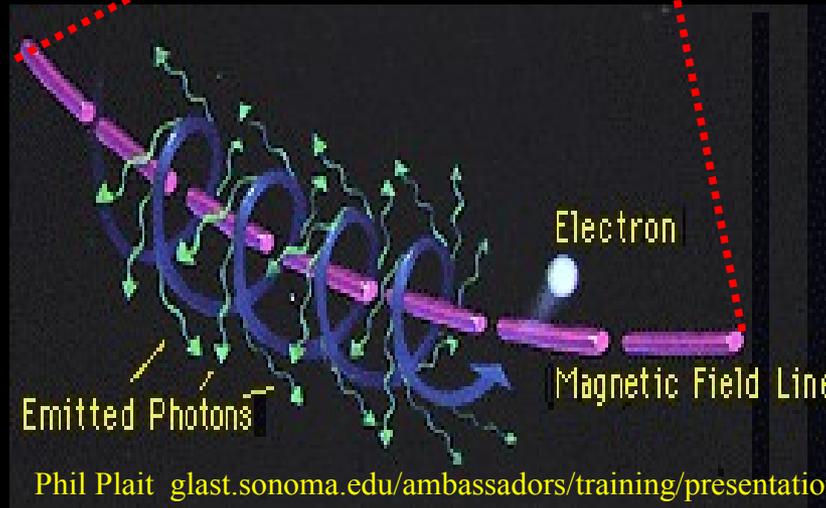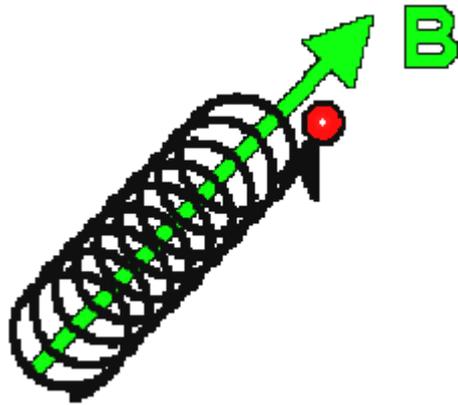
The Lorentz force acts perpendicularly to the magnetic field and bends the particle motion, thus leading to circulation (electrons in clockwise, and ions in anti-clockwise sense) about the field -> **gyromotion** at the gyro- or cyclotron frequency:

$$\omega_g = \frac{qB}{m}$$

When the electron velocity is nonrelativisitic (*v<<c* or *γ-1<<1*) the radiation pattern is just the dipole pattern.
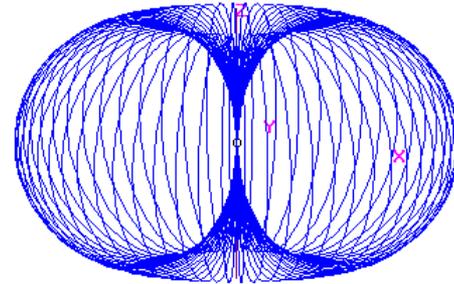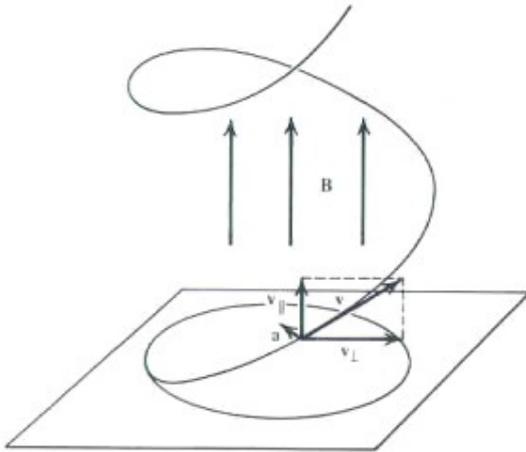
When the electron is relativistic (*v~c* or *γ>>1*) we have, i

Strongly forward peaked!

What this means is that an observer sees a signal which becomes more and more sharply pulsed as the electron increases its speed (and therefore its energy).


T. S. Bastian
NRAO
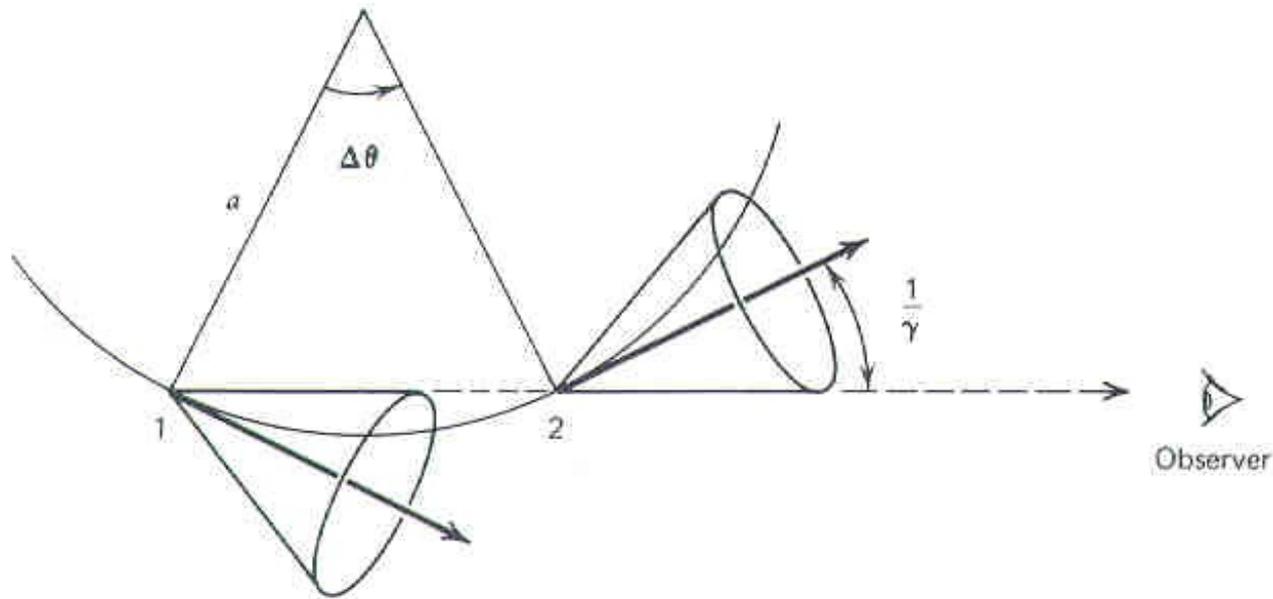
For a nonrelativistic electron, a sinusoidally varying electric field is seen which has a period $2\pi/\Omega_{Be}$,
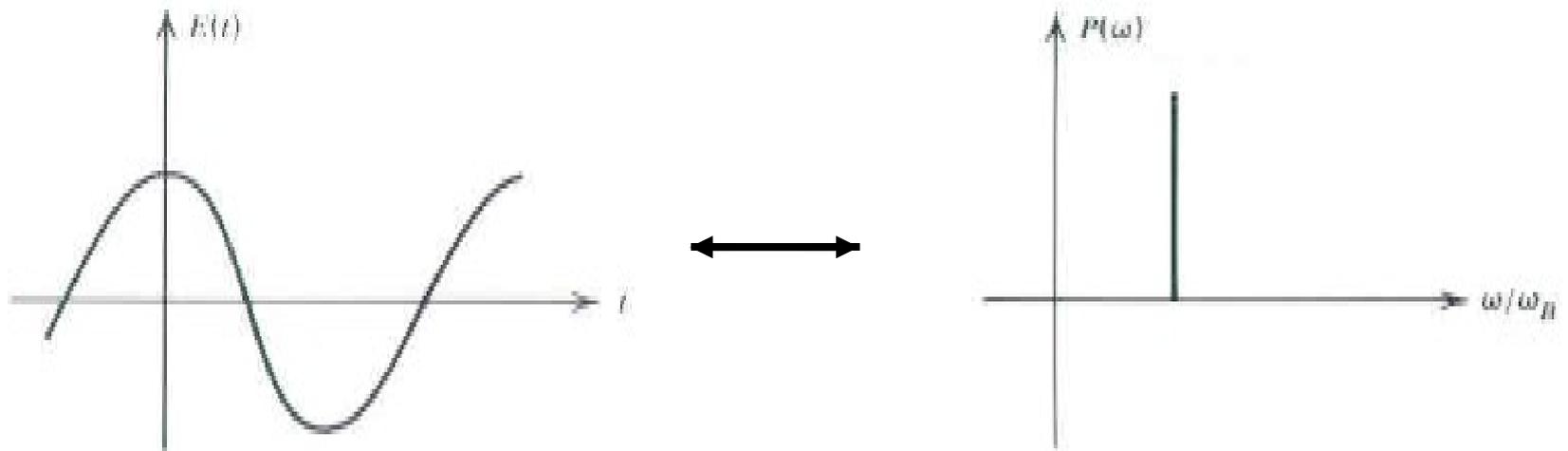
And the power spectrum yields a single tone (corresponding to the electron gyrofrequency).

As the electron energy increases, mild beaming begins and the observed variation of the electric field with time becomes non-sinusoidal.
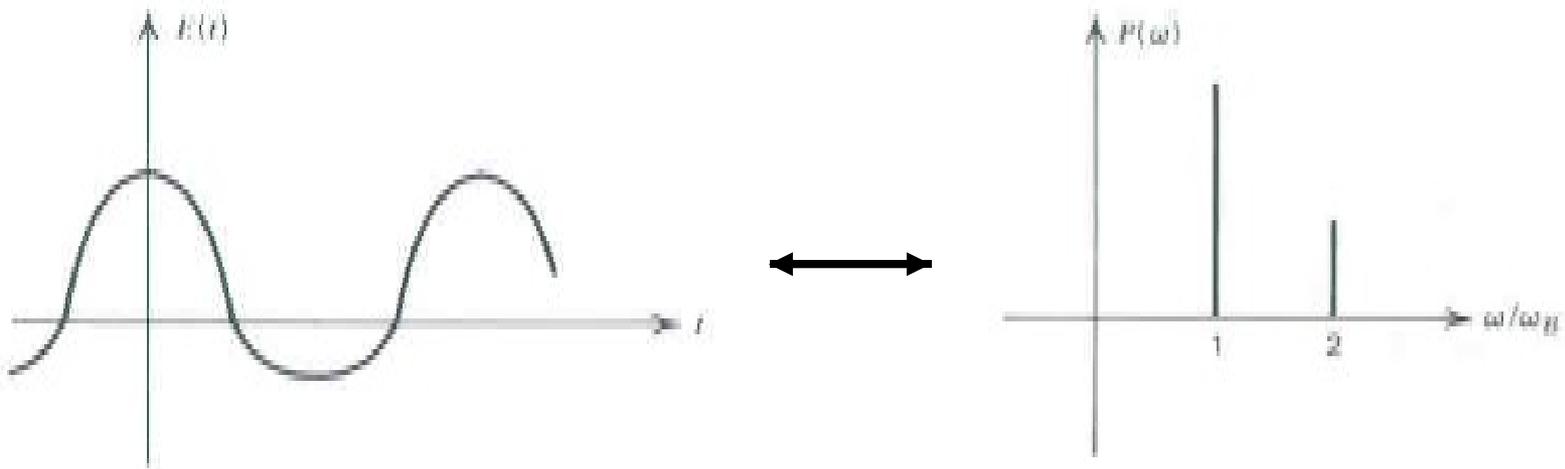
The power spectrum shows power in low harmonics (integer multiples) of the electron gyrofrequency.

Gyroemission at low harmonics of the gyrofrequency is called cyclotron radiation or gyroresonance emission.

When the electron is relativistic the time variation of E is highly non-sinusoidal...
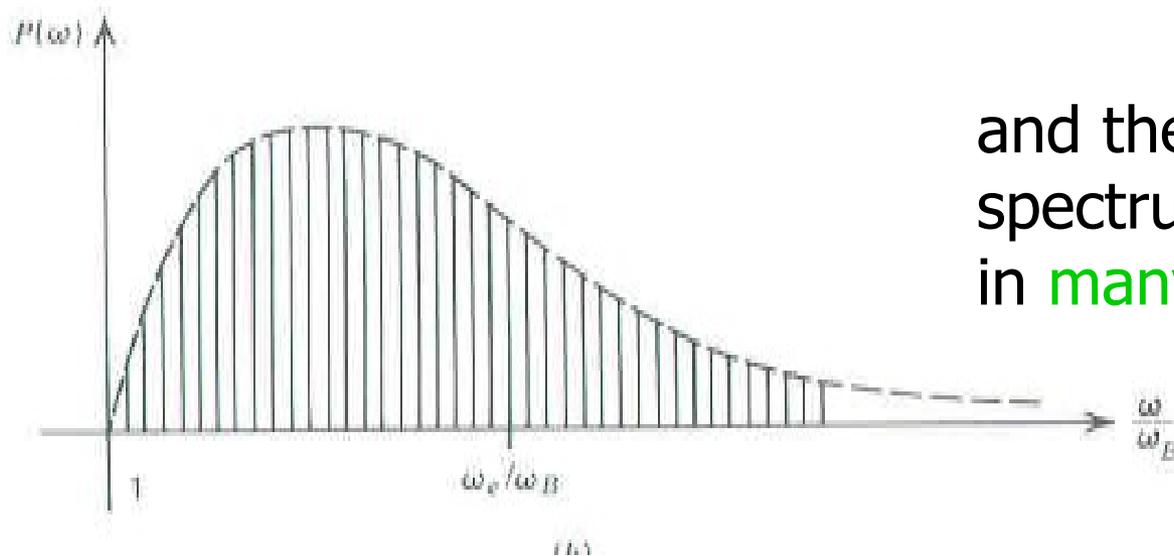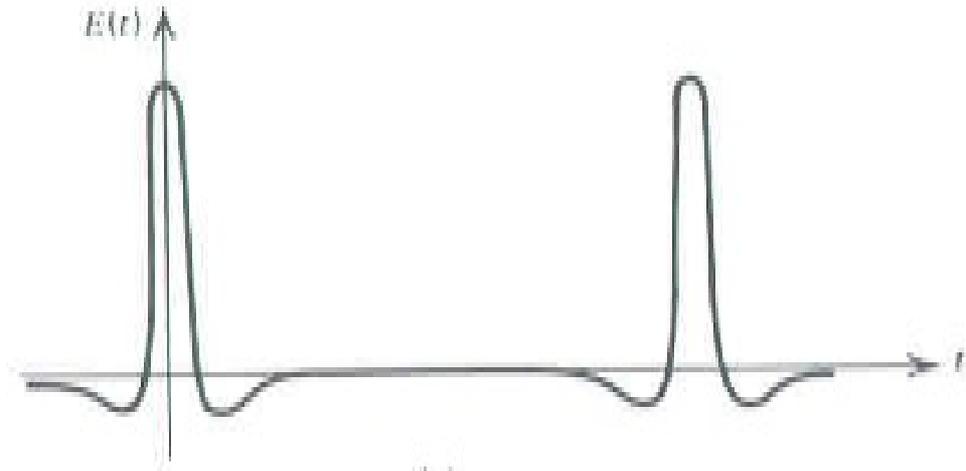
and the power spectrum shows power in many harmonics.

A detailed treatment of the spectral and angular characteristics of electron gyroemission requires a great deal of care.

A precise expression for the emission coefficient that is valid for all electron energies is not available. Instead, expression are derived for various electron energy regimes:

Non-relativistic: $\gamma-1<<1$ (thermal)

cyclotron or gyroresonance radiation

Mildly relativisitic: $\gamma-1\sim1-5$ (thermal/non-thermal)

gyrosynchrotron radiation

Ultra-relativisitic: $\gamma-1>>1$ (non-thermal)

synchrotron radiation

I = J/k (1- exp(-tau))   J,k of 1 electron

1. emissivity/absorption   physic. Process

2.   one electron------->   Population
           electron density energy distribution   N(E)

Synchrotron

The electrons involved are "non-thermal " i.e., with
power law energy distribution:

$$N(E)dE = CE^{-p}dE$$

Sun at
17 GHz

Nobeyama RH

I = J/k (1- exp(-tau))
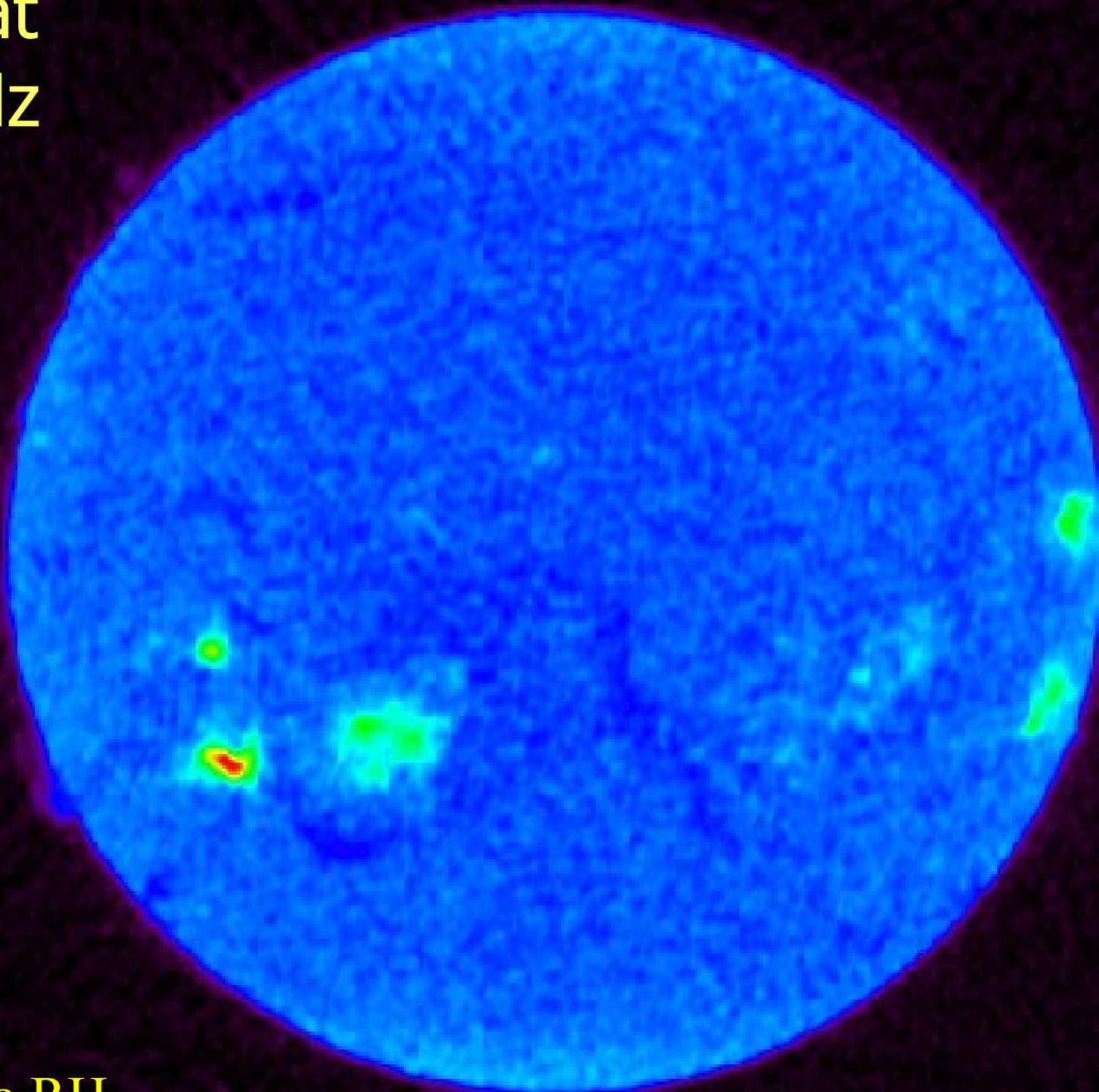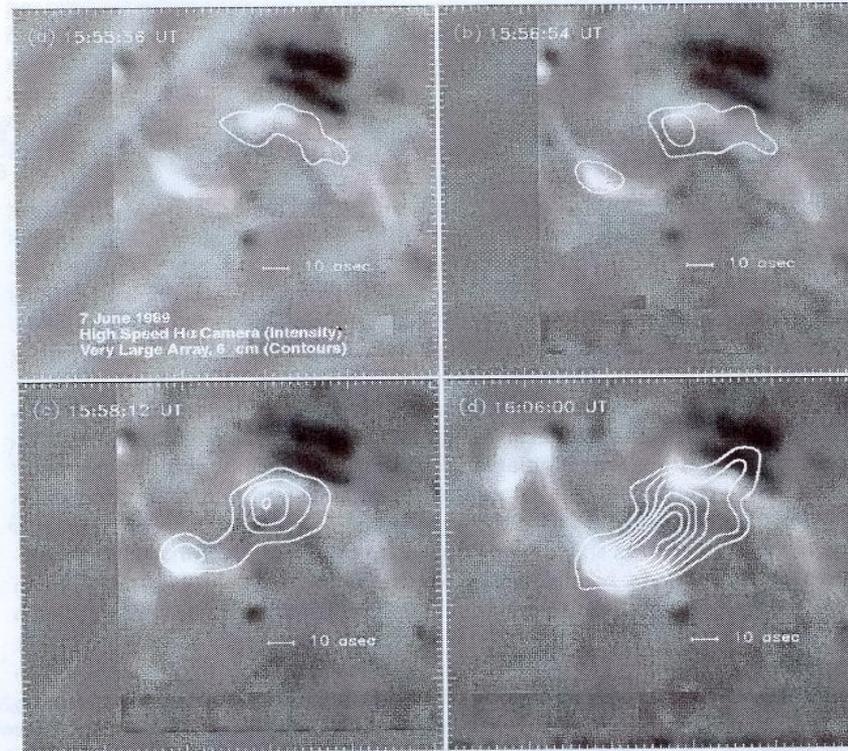

Figure 2 Example of the time evolution of a flaring source at cm-λ. The *contours* represent 4.9-GHz (λ = 6.1 cm) VLA observations of the M8.7 flare in AR 5528 studied by Bastian & Kiplinger (1991). The *gray scale image* shows the Hα emission, characterized by two ribbons. Large sunspots are seen to the northwest. (*a*) In the early phase of the flare, the region containing the strongest magnetic fields emits. (*b*) The magnetically conjugate footpoint then emits. (*c*) The 4.9-GHz emission bridges the magnetic neutral line. (*d*) The entire 4.9-GHz source is optically thick near the time of the flare maximum, and the location of maximum radio brightness lies between the magnetic footpoints.

Bastian & Kiplinger 1991, Alissandrakis et al 1993, Wang et al 1995, Kundu et al 1995a, Hanaoka 1996, 1997, Nishio et al 1997).

The polarization structure of the simulated coronal magnetic loop is not shown in Figure 1. At low frequencies, the source is very optically thick except at its edges, where the assumed number density of energetic electrons is small. The optically thick core of the inhomogeneous source is essentially unpolarized where θ, the angle between the wave normal and the magnetic field vector, is

17 GHz

B gram

SXR

λ

$B \cdot s$

$\tau_g = B \cdot s / c$

s

B

Amplifier

v_1 Voltage Multiplier v_2

τ_i

Integrator

Correlator

Visibility

Amplitude

1.0

0.5

0

Phase

$u \rightarrow$

k_1 / x_a

I-map (ACTIVE REGION)

V-map (ACTIVE REGION)
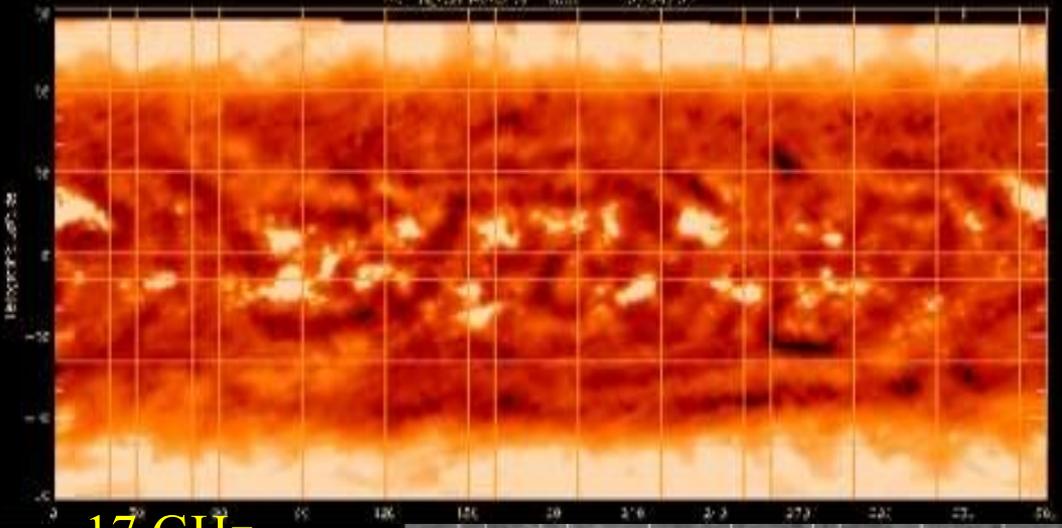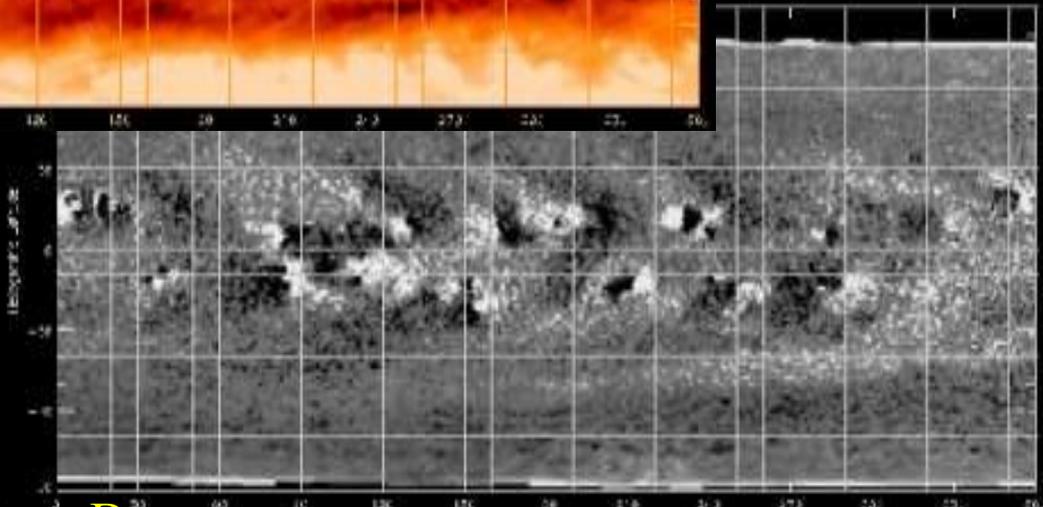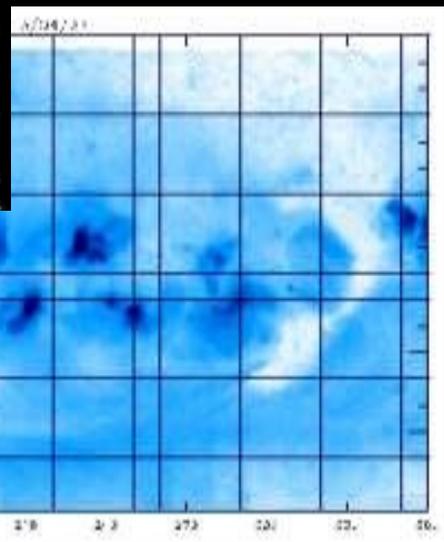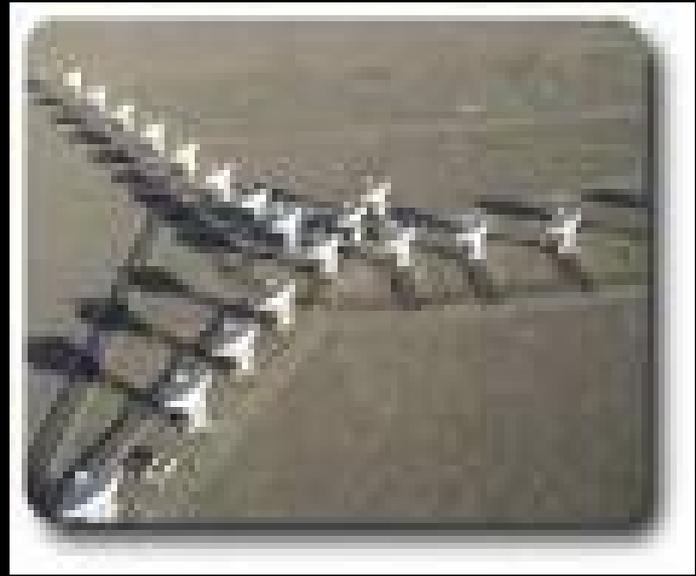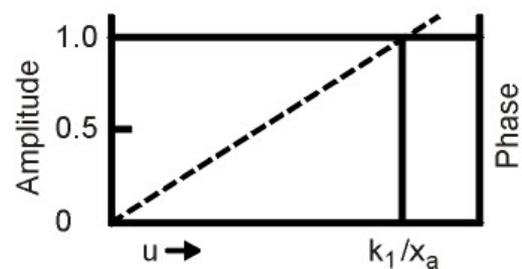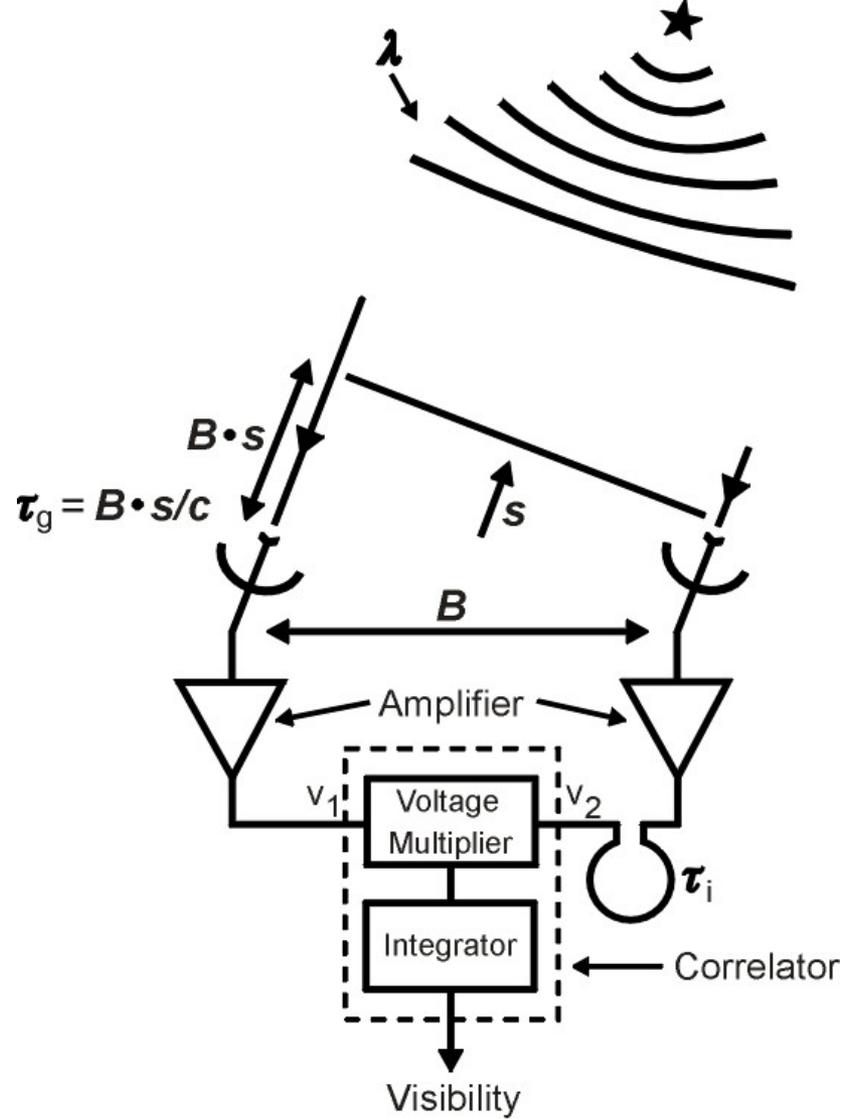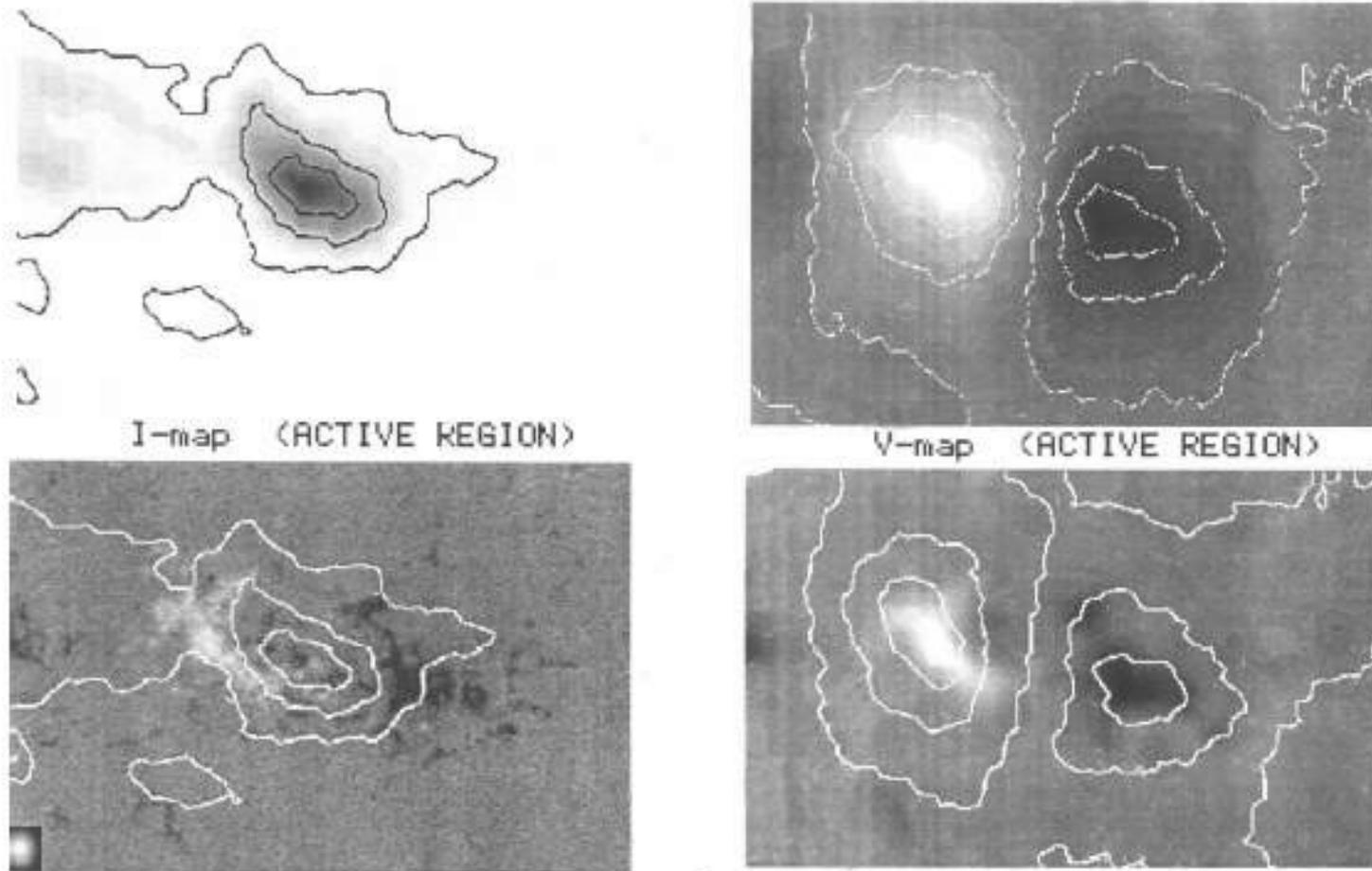
*Figure 5.1.*   Radio maps of the AR observed on June 09, 1995 using Nobeyama radio heliograph at $\lambda = 1.76cm$. Contours present the brightness distribution . Maximum in I channel ($T_b = 27 \cdot 10^3 K$). Maximum in V-channel $T_b^V = 440K$. Maximum degree of polarization $P = 2.8\%$. The region maps are overlapped by gray scale magnetograms . For V-maps they are averaged by the scale of the Nobeyama radio heliograph beam (shown below on the left). The upper V-map present brightness T_b^V, the lower one - percentage $P\%$ of polarization.

Gelfriekh 2004

Magnetic field lines of force

Optical image

Radio emission layers: ▦ 5 GHz ▦ 8 GHz ▦ 11 GHz

Height [arc sec]

Horizontal distance [arc sec]
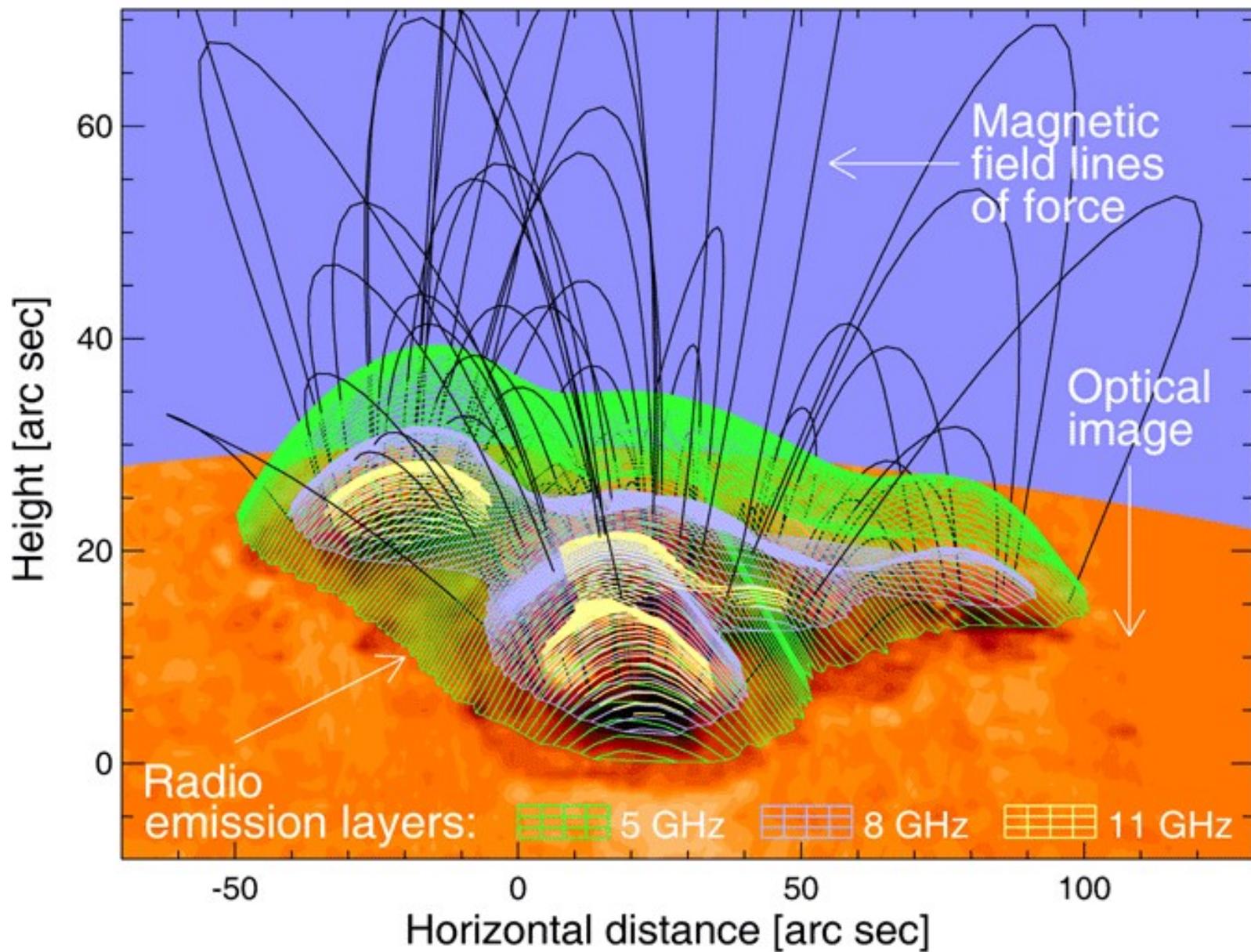
A Schematic Model
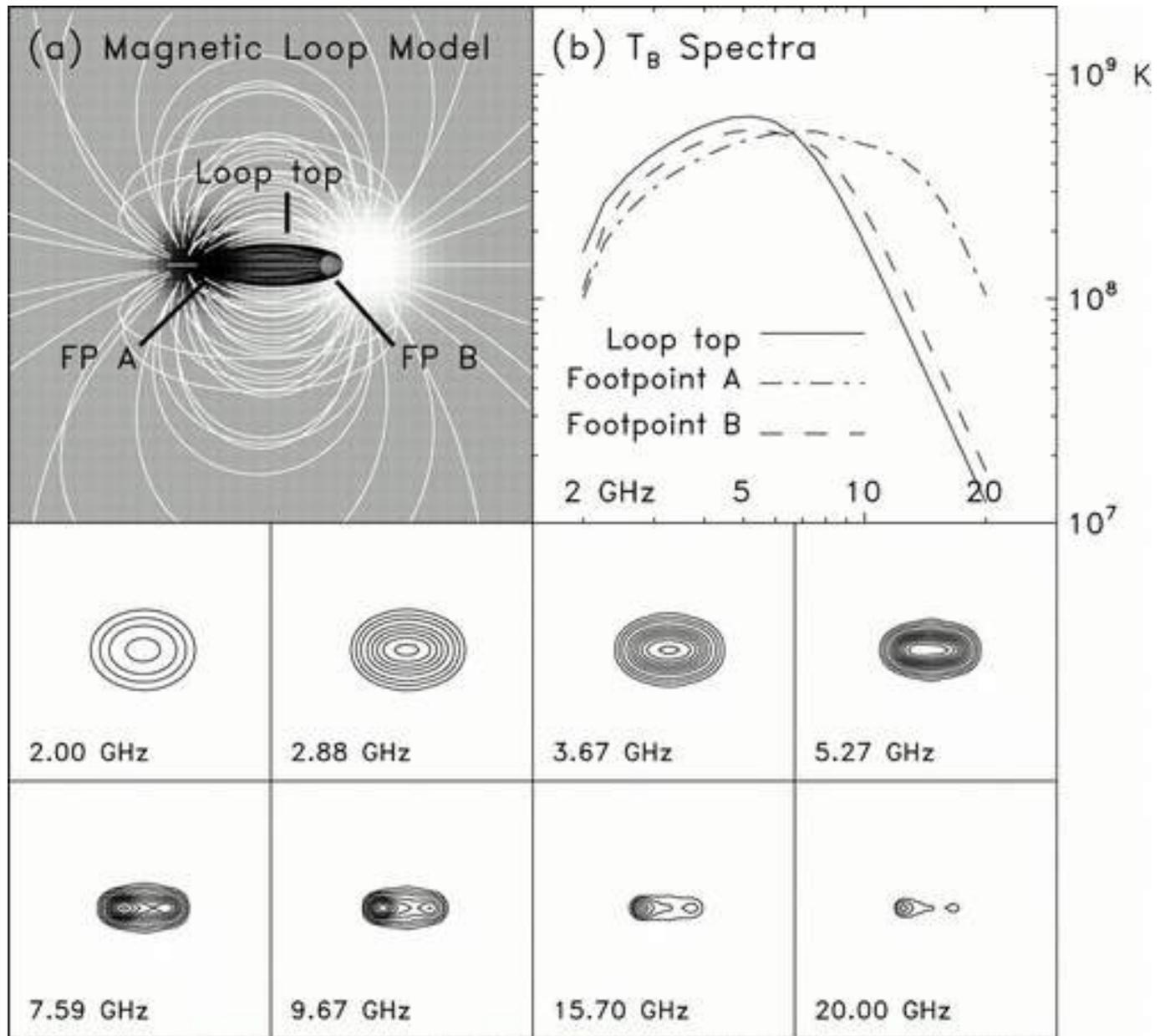
Bastian et al 1998

Nonuniform magnetic fields in space

Shear, twist

Curvature

Divergence

Gradient
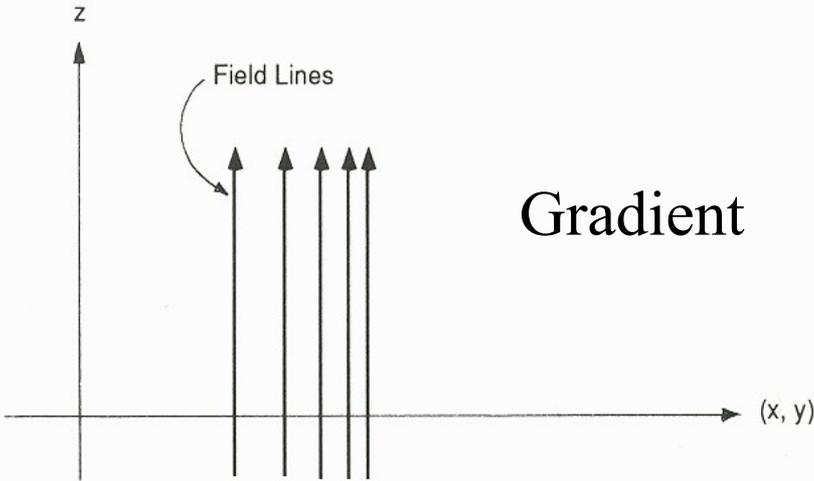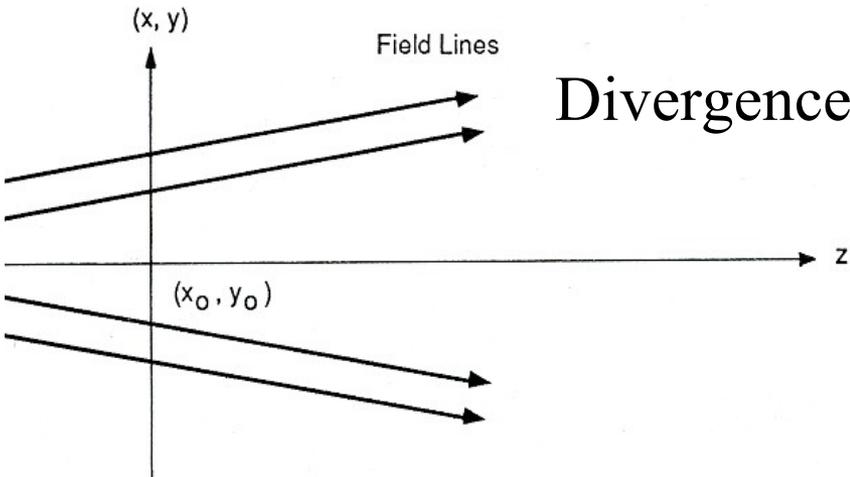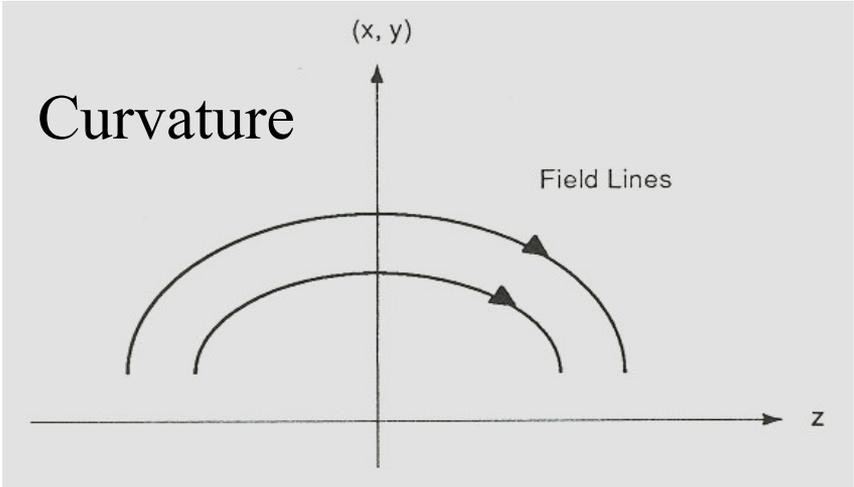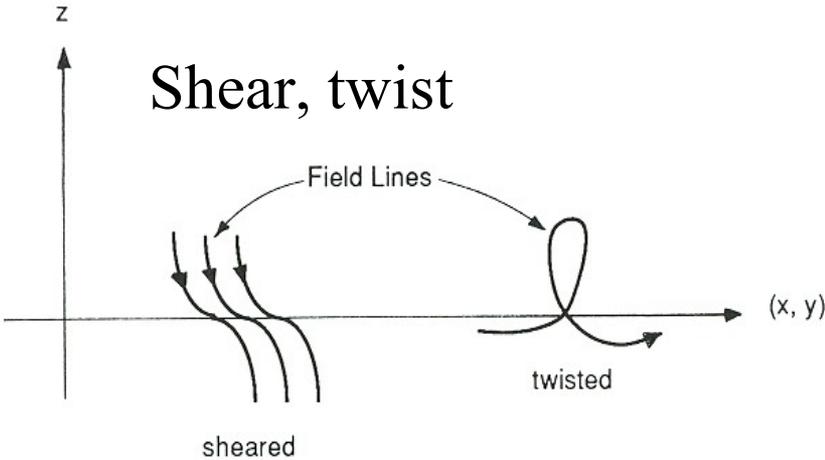
Gyration of ions and electrons III

Helicoidal ion orbit in a uniform magnetic field
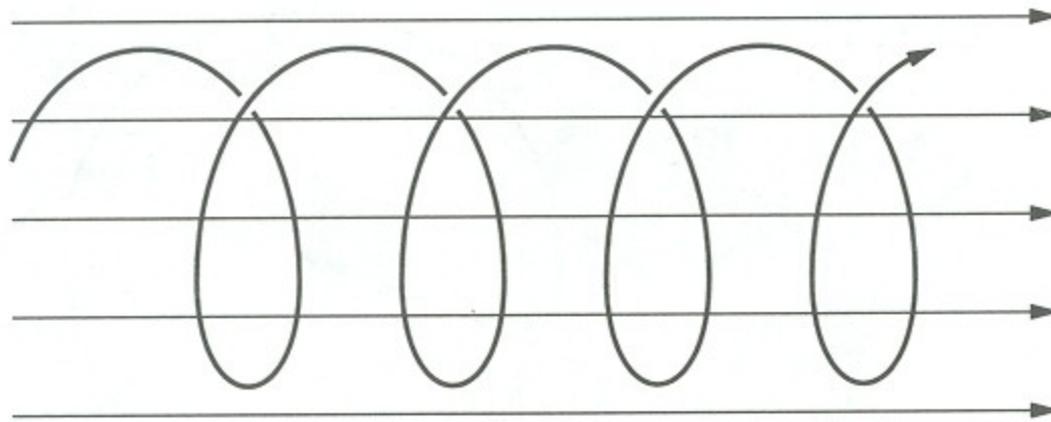
$$r_g = \frac{v_\perp}{|\omega_g|} = \frac{mv_\perp}{|q|B}$$

$$\alpha = \tan^{-1}\left(\frac{v_\perp}{v_\parallel}\right)$$

If one includes a constant speed parallel to the field, the particle motion is three-dimensional and looks like a *helix*. The *pitch angle* of the helix or particle velocity with respect to the field depends on the ratio of perpendicular to parallel velocity components.

Basic definitions: Pitch angle
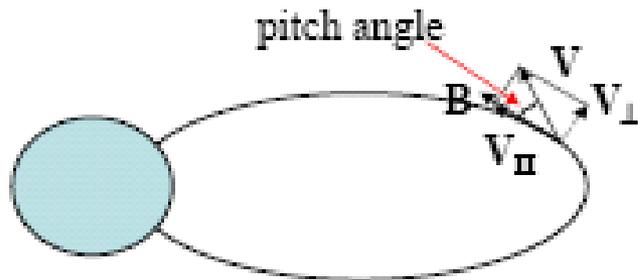
pitch angle

Pitch angle:
Angle between particle velocity vector and magnetic field vector

$$\alpha = \tan^{-1}\left(\frac{V_\perp}{V_{II}}\right)$$

Magnetic moment of particle:

$$\mu = \frac{mv^2 \sin^2 \alpha}{2B} = const$$

Pitch angles of a particle at different locations are directly related to magnetic field at those locations:

$$\frac{\sin^2 \alpha_2}{\sin^2 \alpha_1} = \frac{B_2}{B_1}$$

Natalia Ganushkina (FMI)

Basic definitions: Mirror points

In magnetospheric magnetic field particle moves along magnetic field line:
- Moving into regions of stronger field
- Pitch angle increases
- Transverse energy increases but
  parallel energy decreases

At B_m point, where pitch angles
reaches 90°:
- All energy is in transverse energy,
- Particle cannot penetrate any further
- Particle is reflected and pushed back
along field line

Particle's pitch angle at a specific location is defined by the ratio between the field strength
at that location and at its mirror point

$$\frac{\sin^2 \alpha_2}{\sin^2 \alpha_1} = \frac{B_2}{B_1} \implies \sin \alpha = \left(\frac{B}{B_m} \right)^{1/2}$$

Natalia Ganushkina (FMI)

Basic definitions: Bounce motion

Equatorial pitch angle:

$$\sin^2 \alpha_{eq} = \frac{B_{eq}}{B_m}$$

Basic Components of Particle Motion: bounce, gyration and drift

Flux Tube

Trapped Particle Trajectory

Mirror Point (Pitch angle ~90)

Electron Drift

Magnetic Field Line
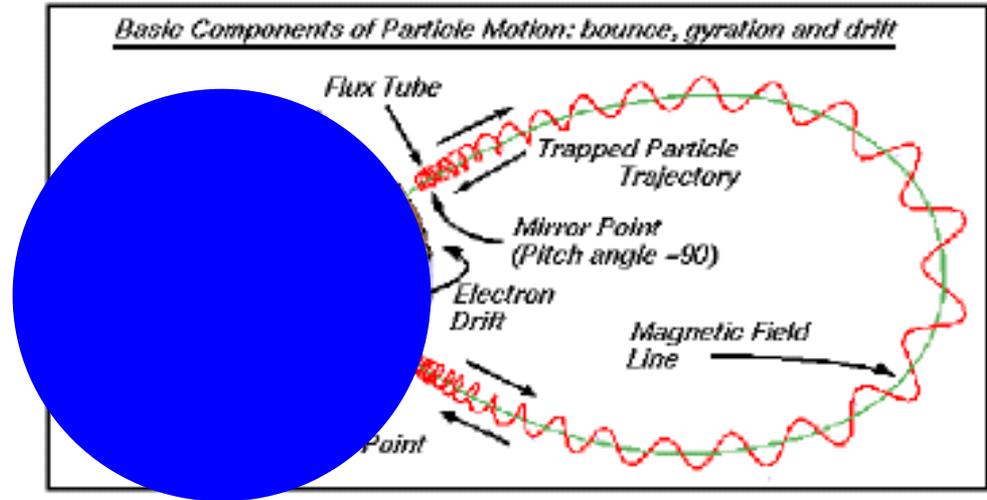
Point

Bounce period, τ_b, is the time it takes a particle to move back and forth between the two mirror points.

Natalia Ganushkina (FMI)

Basic definitions: Loss cone

Not all particles are trapped e

loss cone:

$$\sin^2 \alpha_l = \frac{B}{B_E} \cdot \frac{1}{2}$$

All particles with **pitch angles** $\alpha < \alpha_l$ within the solid
angle $d\Omega$ will be lost
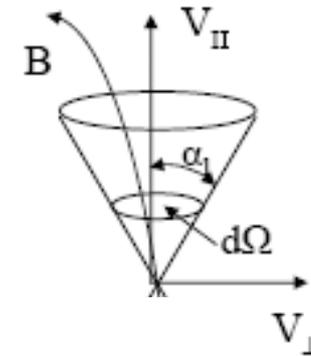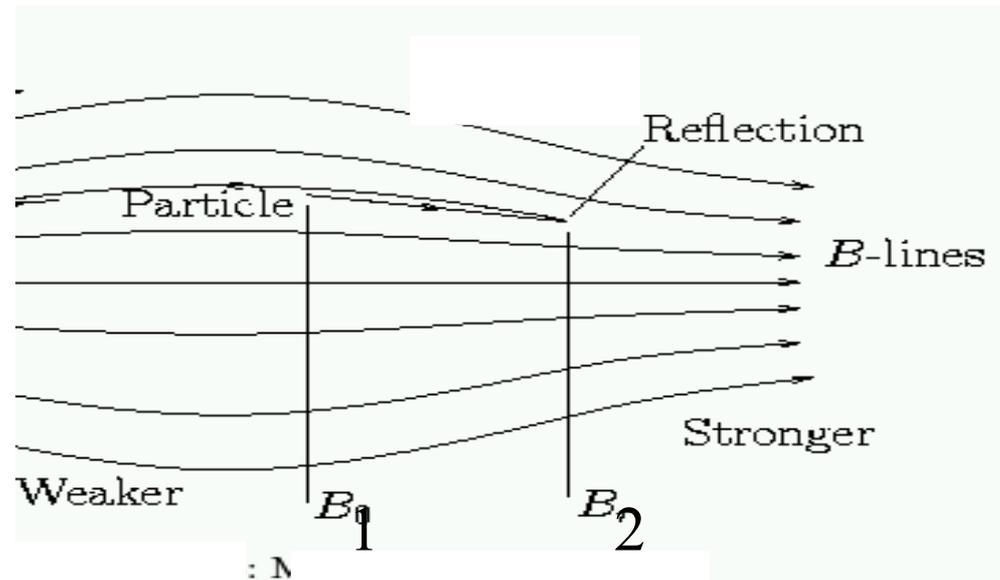
In the context of the standard model:...

as the elcctrons travel along closed magnetic fields, those with
<u>large</u> pitch angles and sufficient energy
(several hundred keV) lose their energy as gyrosynchrotron
radiation
the others reach the chromospere. Their collision with the
dense plasma reveals itself by nonthermal hard X-ray radiation
(HXR, typically between 10-100 keV).

Hard X-ray Flares

Bremsstrahlung Spectrum

- Bremsstrahlung emission (German word meaning "braking radiation")
  - the radiation is produced as the electrons are deflected in the Coulomb field of the ions.
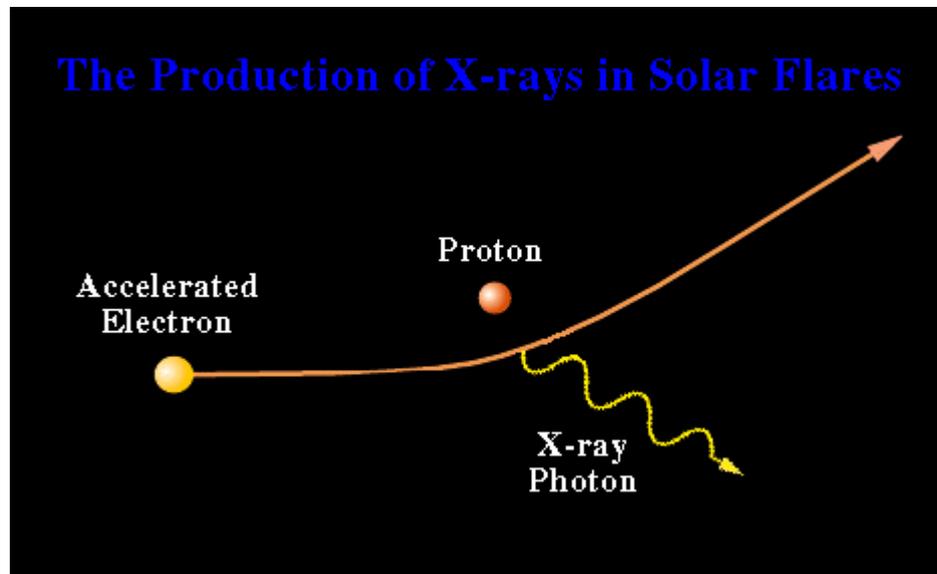
Bremsstrahlung emission

Thick-target bremsstrahlung occurs when an electron enters a thick material, loses energy by multiple collisions with the atoms and electrons in the material, and may eventually come to rest.

The rapid deposition of nonthermal kinetic energy causes an explosive pressure increase in the chromosphere such that heated material "evaporates" into the corona (e.g., Antonucci, Gabriel, & Dennis 1984).
This "chromospheric evaporation" flare scenario is observationally well supported for the Sun. The most compelling evidence for significant heating by nonthermal energy deposition is provided by the "Neupert effect". It manifests itself in a close similarity between the **temporal integral of the hard X-ray lightcurve** and **the soft X-ray lightcurv**e (describing the accumulated thermal energy in the hot plasma).

T

2 – 12 Å X- RAYS

NT

> 50 keV X - RAYS

> 200 keV X - RAYS

0   30   60   90   120 min
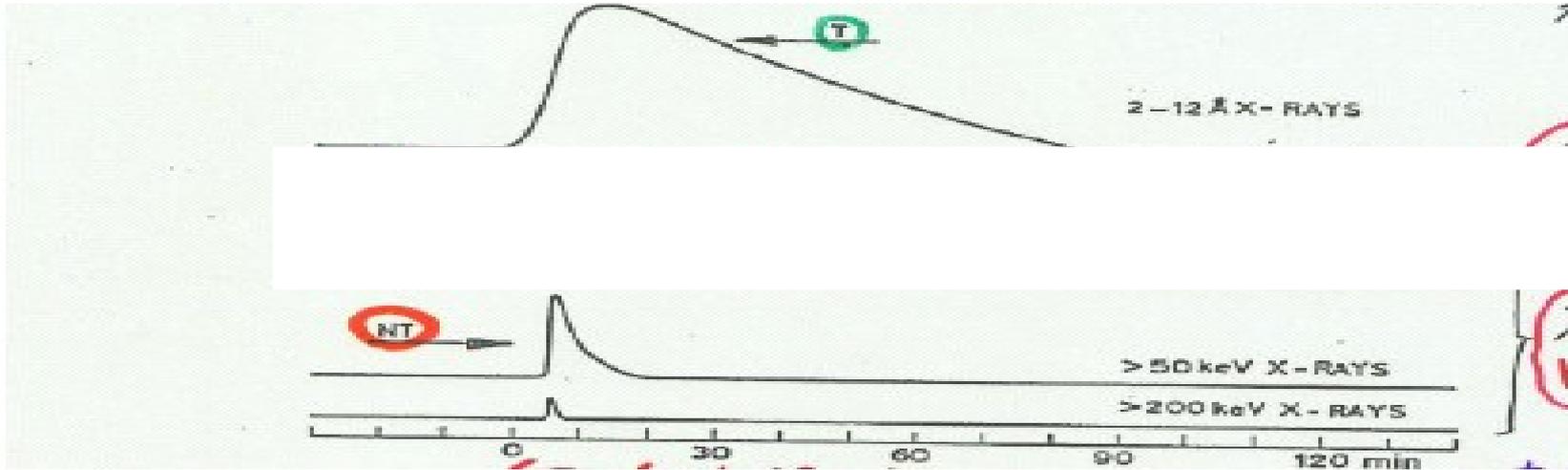
The 'standard' thick-target flare model

Preceding the flare, an Hα prominence (or filament) is activated, becomes unstable and starts to rise.

Following its eruption the opened magnetic field lines reconnect below.

Particles are accelerated, the <u>reconnection jet collides</u> with the SXR loop below producing an MHD fast shock producing the HXR <u>loop-top</u> source and further acceleration.

Electrons and ions stream <u>down the legs </u>of the loop producing HXR emission when they meet the dense chromosphere.

Other features of the thick-target model

- Chromospheric material is heated so rapidly that energy cannot be radiated away; plasma expands to fill the SXR loops.

- As the reconnection proceeds, more and more field lines reconnect producing an arcade of loops seen in SXR.

- The flare footpoints seen in Hα as ribbons can be seen to move apart. Similar motion seen at HXR footpoints.

Flare Model

- Hard X-ray source appear at the top of the loop
- Compact hard X-ray sources appear at two footpoints of soft X-ray loop
- Coronal loop structure of soft X-ray
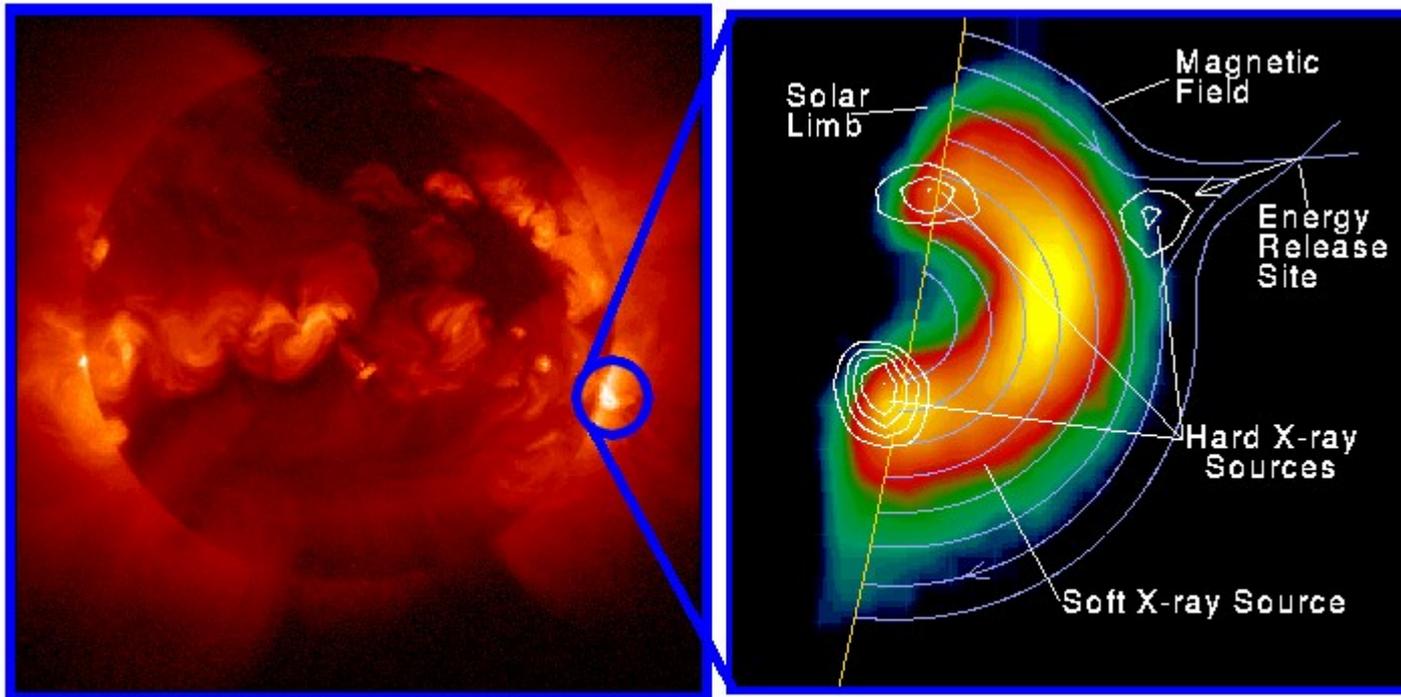
Yohkoh X-ray Image of a Solar Flare, Combined Image in Soft X-rays (left) and Soft X-rays with Hard X-ray Contours (right). Jan 13, 1992.

SPECTRA

$$I = J/k \ (1 - \exp(-\text{tau}))$$

1. emissivity/absorption   physic. Process
2.   one electron------->   Population
           electron density energy distribution   N(E)

3. If unresolved:

   Integral over source solid angle... $(\text{size/distance})^2$
    Flux density   S
   Spectrum: S   vs   frequency

$$N(E)dE = CE^{-p}dE$$

In this case, we have

$$S(\nu) \propto \nu^{-\frac{p-1}{2}}$$

Flux density (Jy)
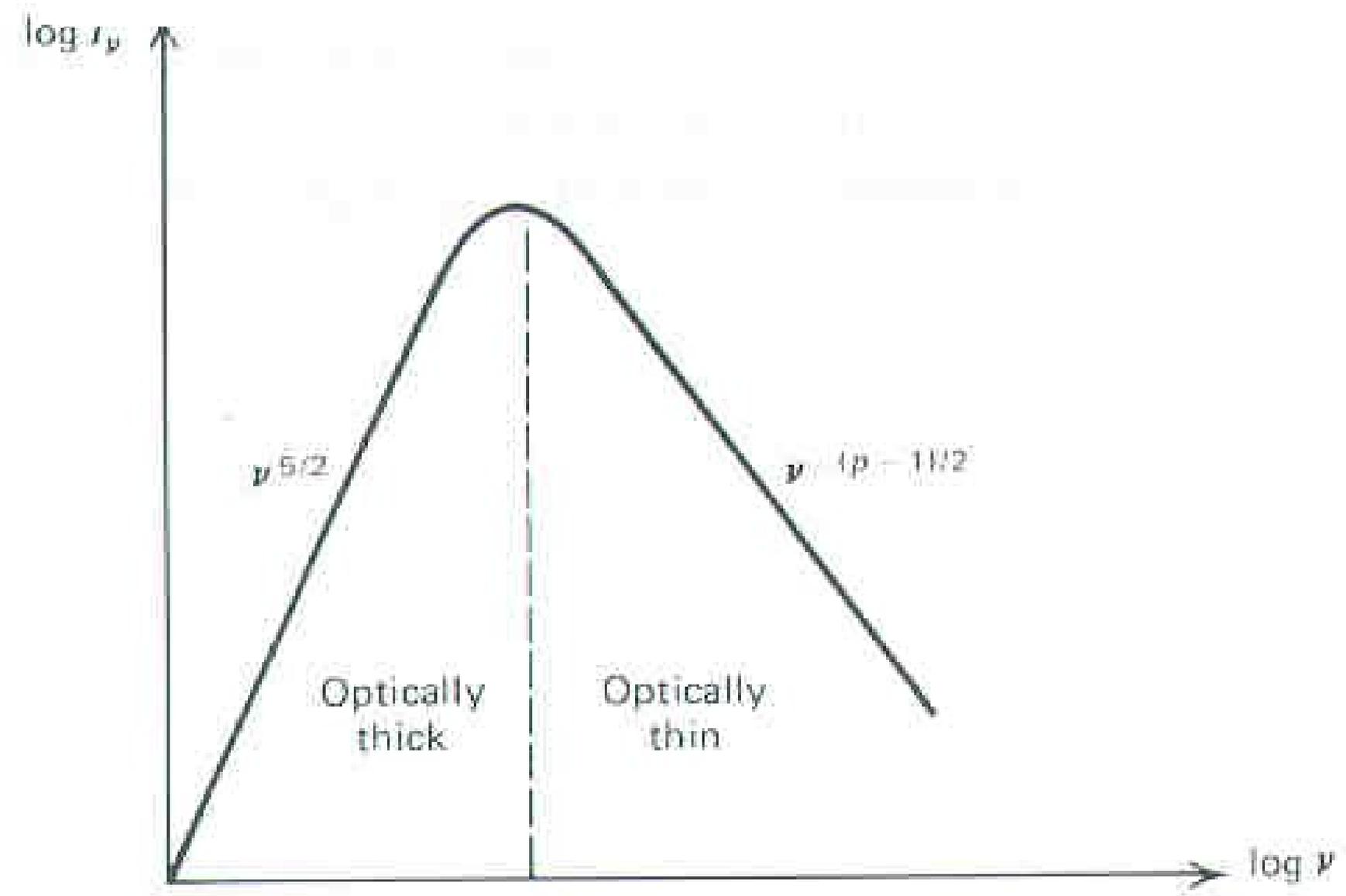
- Radio astronomers express flux density in units of Janskys

$$1 \text{ Jy} = 10^{-26} \text{ W m}^{-2} \text{ Hz}^{-1}$$

- Solar radio physics tends to employ solar flux units (SFU)

$$1 \text{ SFU} = 10^4 \text{ Jy}$$

- While specific intensity can be expressed in units of Jy/beam or SFU/beam, a simple and intuitive alternative is brightness temperature, which has units of Kelvin.

Variation with B
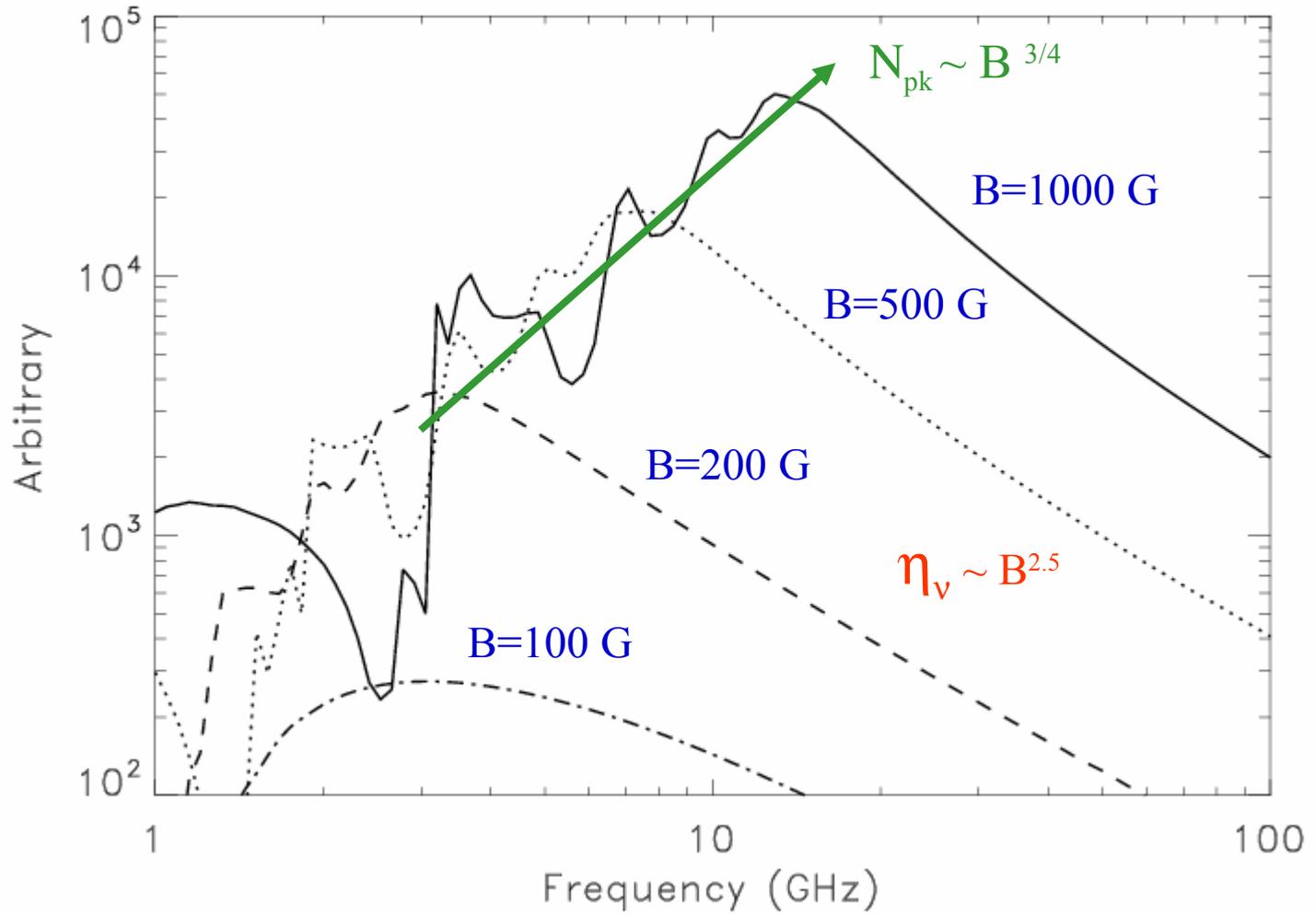
The flare's hard X-ray spectrum

The HXR spectrum can be described by a power law:

$$\frac{dI(E)}{dE} = CE^{-\gamma} \quad \text{photons m}^{-2}\,\text{s}^{-1}\,\text{keV}^{-1}$$

where $I(E)$ is the measured photon flux and γ is the spectral hardness where $2.5 < \gamma < 5.0$ usually. The spectral constant C ranges between 10^3-10^7, increasing with higher values of γ.
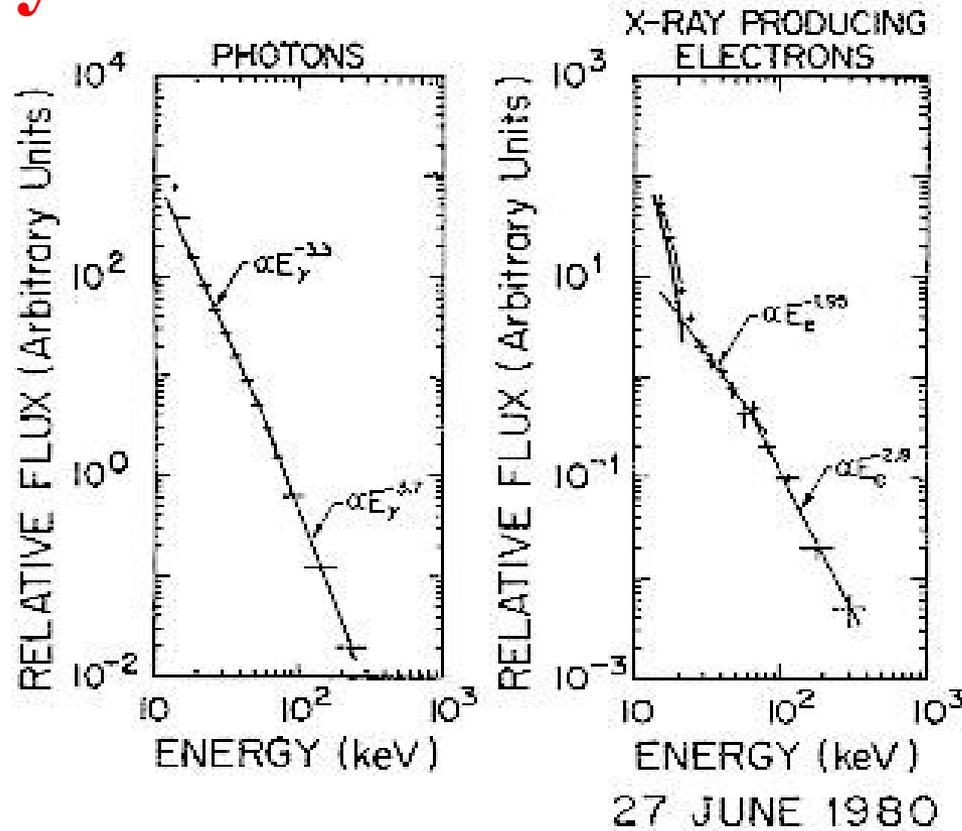
X-ray flares

Hard X-ray flare spectrum with derived spectra of the X-ray producing electrons (Johns & Lin, 1992)

Flare: Spectrum

- The emission spectrum during flare's impulsive phase

Composite Solar Flare Spectrum

Flare: Spectrum
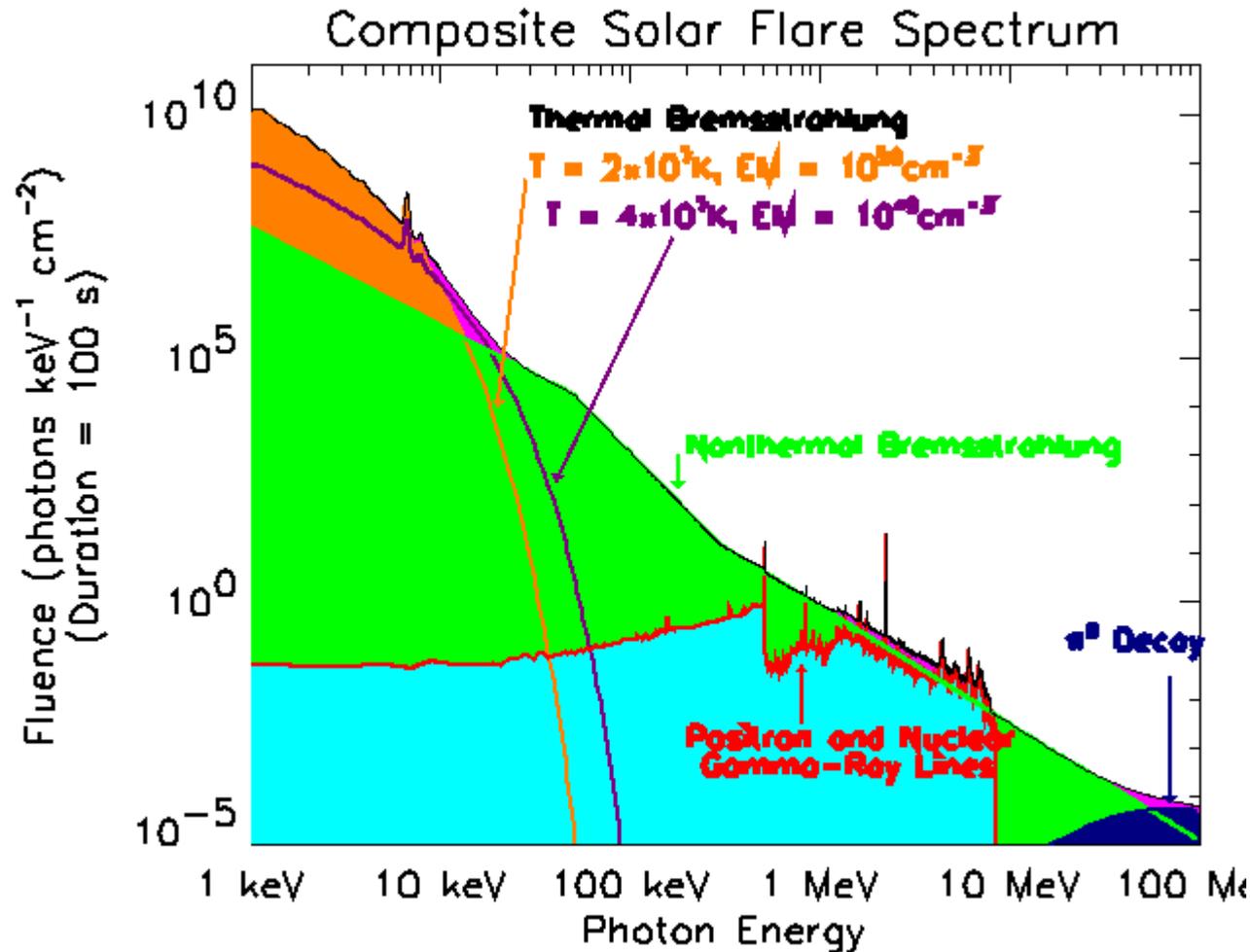
Composite Solar Flare Spectrum

- A full flare spectrum may have three components:
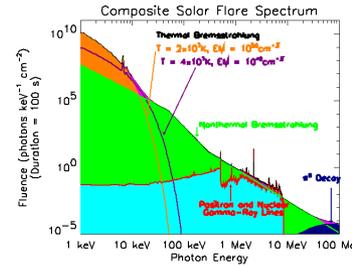
1. Exponential distribution in Soft X-ray energy range (e.g., 1 keV to 10 keV):
   - thermal Bremsstrahlung emission

3. Power-law distribution in hard X-ray energy range (e.g., 10 keV to 100 keV):
   - non-thermal Bremstrahlung emission
   - $dF(E)/dE = AE^{-\gamma}$ Photons cm^{-2} s^{-1} keV^{-1}
     Where γ is the power-law index

4. Power-law plus spectral line distribution in Gamma-ray energy range (e.g., 100 keV to 100 MeV)
   - non-thermal Bremstrahlung emission
   - Nuclear reaction

OSSE SPECTRUM OF THE 1991 JUNE 4 SOLAR FLARE

α–α line ⇨
{ • high α/p or ambient ^{4}He
  • particles not beamed }

annihilation radiation ⇨ $\rho > 10^{13}$ cm^{-3}

α–Fe line ⇨ low ambient ^{4}He

Spectral variability ⇨ physics of particle acceleration

Mg, Si, Fe ⇨ coronal ambient composition ⇦ C & O

n capture ⇨ photospheric ^{3}He

broad nuclear lines ⇨ accelerated particle abundances

nuclear bremsstrahlung ⇨
{ accelerated ion energy > electron energy }

Ne/O ⇨ steep particle spectrum